

FULL PAPER

Design, synthesis, and biological evaluation of novel benzimidazole derivatives as sphingosine kinase 1 inhibitor

Sarah H. M. Khairat¹ | Mohamed A. Omar¹ | Fatma A. F. Ragab² | Sonam Roy³ | Ahmad A. Turab Naqvi⁴ | Ahmed S. Abdelsamie^{1,5} | Anna K. H. Hirsch^{5,6} | Shadia A. Galal¹  | Md. Imtaiyaz Hassan³ | Hoda I. El Diwani¹ 

¹Department of Chemistry of Natural and Microbial Products, Division of Pharmaceutical and Drug Industries Research, National Research Centre, Cairo, Egypt

²Department of Pharmaceutical Chemistry, Faculty of Pharmacy, Cairo University, Cairo, Egypt

³Centre for Interdisciplinary Research in Basic Sciences, Jamia Millia Islamia, New Delhi, India

⁴Department of Drug Design and Optimization, Helmholtz Institute for Pharmaceutical Research Saarland (HIPS), Helmholtz Centre for Infection Research (HZI), Saarbrücken, Germany

⁵Department of Pharmacy, Saarland University, Saarbrücken, Germany

⁶Department of Pharmaceutical Chemistry, Faculty of Pharmacy, Cairo University, Cairo, Egypt

Correspondence

Shadia A. Galal, Department of Chemistry of Natural and Microbial Products, Division of Pharmaceutical and Drug Industries Research, National Research Centre, El Buhouth St., Dokki, P.O. Box 12622, Cairo, Egypt.

Email: sh12galal@hotmail.com

Md. Imtaiyaz Hassan, Centre for Interdisciplinary Research in Basic Sciences, Jamia Millia Islamia, New Delhi 110025, India. Email: mihassan@jmi.ac.in

Funding information

Indian Council of Medical Research, Grant/Award Number: ISRM/12(22)/2020

Abstract

Sphingosine kinase 1 (SphK1) has emerged as an attractive drug target for different diseases. Recently, discovered SphK1 inhibitors have been recommended in cancer therapeutics; however, selectivity and potency are great challenges. In this study, a novel series of benzimidazoles was synthesized and evaluated as SphK1 inhibitors. Our design strategy is twofold: It aimed first to study the effect of replacing the 5-position of the benzimidazole ring with a polar carboxylic acid group on the SphK1-inhibitory activity and cytotoxicity. Our second aim was to optimize the structures of the benzimidazoles through the elongation of the chain. The enzyme inhibition potentials against all the synthesized compounds toward SphK1 were evaluated, and the results revealed that most of the studied compounds inhibited SphK1 effectively. The binding affinity of the benzimidazole derivatives toward SphK1 was measured by fluorescence binding and molecular docking. Compounds **33**, **37**, **39**, **41**, **42**, **43**, and **45** showed an appreciable binding affinity. Therefore, the SphK1-inhibitory potentials of compounds **33**, **37**, **39**, **41**, **42**, **43**, and **45** were studied and IC₅₀ values were determined, to reveal high potency. The study showed that these compounds inhibited SphK1 with effective IC₅₀ values. Among the studied compounds, compound **41** was the most effective one with the lowest IC₅₀ value and a high cytotoxicity on a wide spectrum of cell lines. Molecular docking revealed that most of these compounds fit well into the ATP-binding site of SphK1 and form hydrogen bond interactions with catalytically important residues. Overall, the findings suggest the therapeutic potential of benzimidazoles in the clinical management of SphK1-associated diseases.

KEYWORDS

benzimidazole, drug design and discovery, kinase inhibitors, molecular docking, pyrazole, sphingosine kinase 1

1 | INTRODUCTION

Sphingosine kinases (SphK) play a significant role in cancer progression and thus considered as an attractive drug target. Recently, numerous inhibitors of SphK1 were designed, which show significant therapeutic implications (Figure 1). Phosphorylation of D-erythro-sphingosine (**1**) is catalyzed by SphK to produce sphingosine-1-phosphate (S1P, **2**) which is responsible for regulating proliferation, neovascularization, cell survival, and migration through five G-protein-coupled receptors (S1PR1-5).^[1,2] S1P, **2**, being a cellular

signaling molecule, plays an important role in a variety of diseases, for example, cancer,^[3,4] fibrosis,^[5] Alzheimer's disease,^[6] cell disease,^[7,8] and viral infections such as Chikungunya virus.^[9] The key players among sphingolipid metabolites are ceramide, sphingosine, and S1P.^[10,11] The role of ceramide and sphingosine is to be proapoptotic molecules, that is, to mediate the cell cycle and to arrest and induce apoptosis. However, S1P acts as a "pro-survival" molecule and promotes cell proliferation.^[12,13] The balance between intracellular levels of these two oppositely acting sphingolipid metabolites represents a "sphingolipid rheostat," which is crucial in the

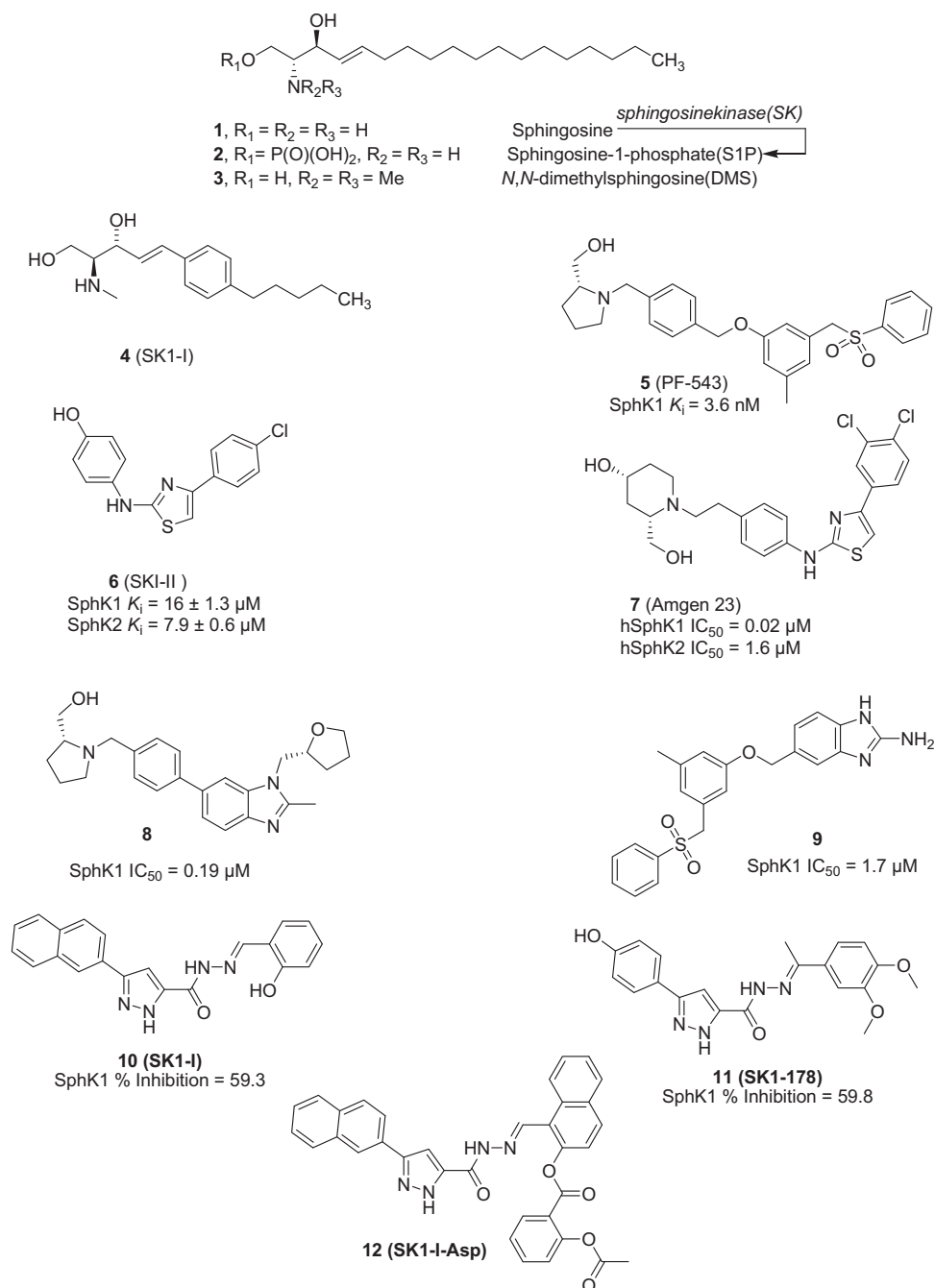


FIGURE 1 Examples of SphK1 inhibitors

determination of the cell fate.^[14] A lean of this balance toward the ceramide side makes the cell destined toward apoptotic or death pathways, whereas cell growth and survival are induced when S1P accumulates within the cell.^[15] Modulation of this rheostat to improve the levels of ceramide or sphingosine and to decrease S1P can be adopted as a therapeutic strategy in cancer treatment.^[16,17] SphK is one of the key regulators of this rheostat, as it generates S1P from sphingosine, thereby decreasing the intracellular levels of both sphingosine and ceramide,^[18,19] which are encoded by different genes and exhibit distinct biochemical properties, subcellular distributions, and substrate and inhibitor sensitivities.^[20]

It was recently found that SphK1 is involved in several human pathologies, including cancer, pulmonary fibrosis, rheumatoid arthritis, asthma, diabetes, and neurodegenerative disorders.^[21,22] Overexpression of SphK1 has been observed in breast, lung, uterus, colon, pancreas, ovary, kidney cancers, and leukemia.^[23-28] In addition, it was reported that SphK1 is essential in processes like tumorigenesis, angiogenesis, and chemotherapy resistance, which are crucial for metastasis and cancer progression.^[21]

A slow down of tumor growth and decrease in the sensitivity of cancer cells to chemotherapeutics are produced by inhibition of SphK1.^[29] Therefore, SphK1 represents a potential target for drug discovery in the treatment of cancer and other diseases.^[30,31] However, the chemotypes of SphK1 inhibitors reported are limited.

Sphingosine analogs, for example, *N,N*-dimethylsphingosine (DMS, **3**) (Figure 1), were discovered as a potent inhibitor of SphK1 and have been used for modulating S1P biosynthesis.^[32] The SK1-selective inhibitor (SK1-I, **4**) reported by Paugh et al.^[29] reduced the growth and survival of human leukemia U937 cells in vitro and suppressed U937 growth in a murine xenograft model. Fingolimod is phosphorylated by SphK2 to act as a functional antagonist of S1P receptors, S1P1/3.^[33,34]

Potent SphK1-selective inhibitors and SphK1/SphK2 dual inhibitors (**5-7**, Figure 1) were reported. The SphK1-selective inhibitor **5** (PF-543)^[35,36] and SphK1/SphK2 dual inhibitor **6** (SKI-II)^[37-40] have been co-crystallized with SphK1 and were used in the discovery of new inhibitors.^[40,41] A selective SphK1 inhibitor, **7** (Amgen 23), was reported.^[42] Benzimidazoles **8** and **9** were reported as inhibitors of S1P formation in cells.^[36] In addition, several SphK inhibitors that possess the pyrazole ring in their structures were also reported as SphK1 inhibitor, for example, compounds **10-12** (Figure 1). The identification of the SphK1-specific analog, SKI-178, that is active in vitro and in vivo was performed.^[43] The discovery of more potent and selective SphK1 inhibitors could lead to a new potential therapy for the treatment of cancer and/or immune-mediated diseases. The benzimidazole moiety is well known to interact with kinases by multiple binding modes.^[44-47]

As a continuation of our research^[48-57] for the synthesis of new benzimidazoles targeting new enzymes, the target of this study was to design and synthesize SphK1 inhibitors by substituting the 5-position of benzimidazole with different groups and studying the effect of these substituents on the inhibitory activity of SphK-1 and its correlation with cytotoxic activity.

The evolution of SphK1 and SphK2 inhibitors has been recently reported.^[58,59] Many SphK inhibitors were designed to have a polar head group and a lipophilic tail region. On the basis of the above facts, two main structural features should be taken into consideration. First, a bulky substitution at the tail increases the potency and selectivity toward SphK-1. Second, substituting the hydroxyl polar head with other polar groups is more preferred. Motivated by the previous information, our design strategy is twofold: it aimed first at replacing the hydroxyl group to prevent its phosphorylation by other polar groups, as acid (COOH), ester (COOC₂H₅), and carbonyl (CONH₂) seem to be important. In addition, increasing lipophilicity by introducing saturated heterocycles to the pyrazole ring as R₂ = morpholinyl, piperidinyl, and pyrrolidinyl in the lipophilic tail, as well as the introduction of a phenyl ring, will enhance the lipophilicity and bioavailability by producing a better drug-like profile.

Its next objective was to optimize the structures of benzimidazoles through elongation of the carbonyl CONH₂ to CONH=CH-C₆H₄OH by reacting with aldehydes to study the effect of the azomethine group (CH=N) on the activity. All these structural modifications are performed to fulfill our target, which is improving the pharmacological properties of the new compounds (Figure 2).

2 | RESULTS AND DISCUSSION

2.1 | Chemistry

This study aimed to synthesize new benzimidazole candidates as SphK1 inhibitors (Figure 2), taking into consideration that polar substitution of the benzimidazole ring at 5-position was essential for activity.^[35] The target benzimidazole derivatives were synthesized as shown in Schemes 1-4. The desired pyrazole **13** has been synthesized by the reaction of ethyl acetoacetate with phenylhydrazine in the presence of ethanol and glacial acetic acid, according to the procedure described by Prajuli et al.^[60] The Vilsmeier-Haack reaction of the previous step afforded 5-chloro-3-methyl-1-phenylpyrazole-4-carboxaldehyde, which was followed by the introduction of nucleophiles, that is, secondary amines or phenol derivatives, to give compounds **15-20**^[61-63] (Scheme 1). Coupling of 3,4-diaminobenzoic acid with substituted pyrazole-4-carboxaldehydes **15-20** in the presence of sodium metabisulfite in ethanol yielded 2-pyrazolylbenzimidazole derivatives **21-26** (Scheme 2). Esterification of compounds **21-26** with ethanol and concentrated sulfuric acid afforded compounds **27-32**, respectively. Subsequently, compounds **27, 28, 30, or 31** were treated with hydrazine hydrate to yield the respective hydrazides **33-36** (Scheme 2). Moreover, compound **33** was condensed with different aldehydes including 4-hydroxybenzaldehyde, 3-hydroxybenzaldehyde, vanillin, 4-chlorobenzaldehyde, or furfural to afford compounds **37-41** respectively (Scheme 3). Finally, compound **35** was condensed with 4-hydroxybenzaldehyde, 3-hydroxybenzaldehyde, vanillin, or

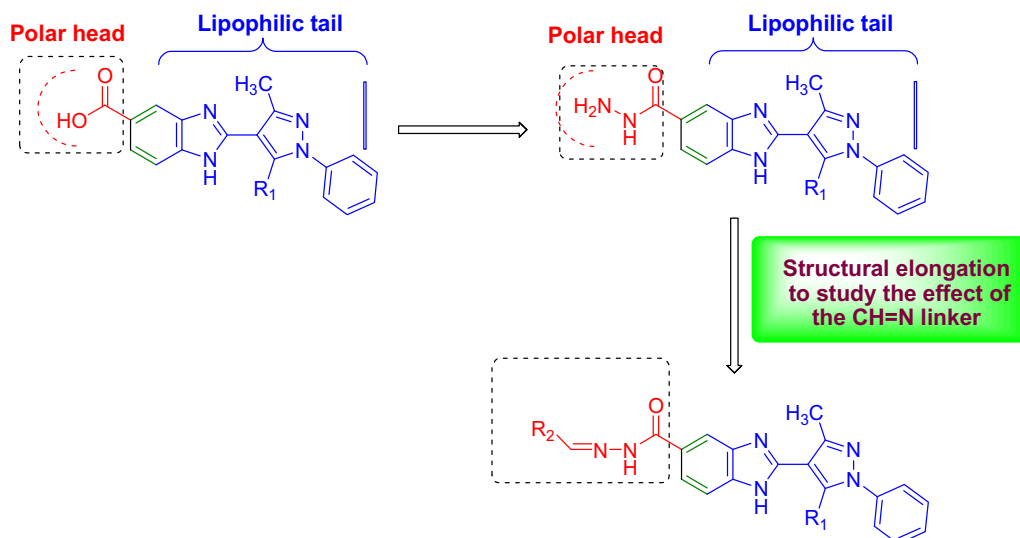
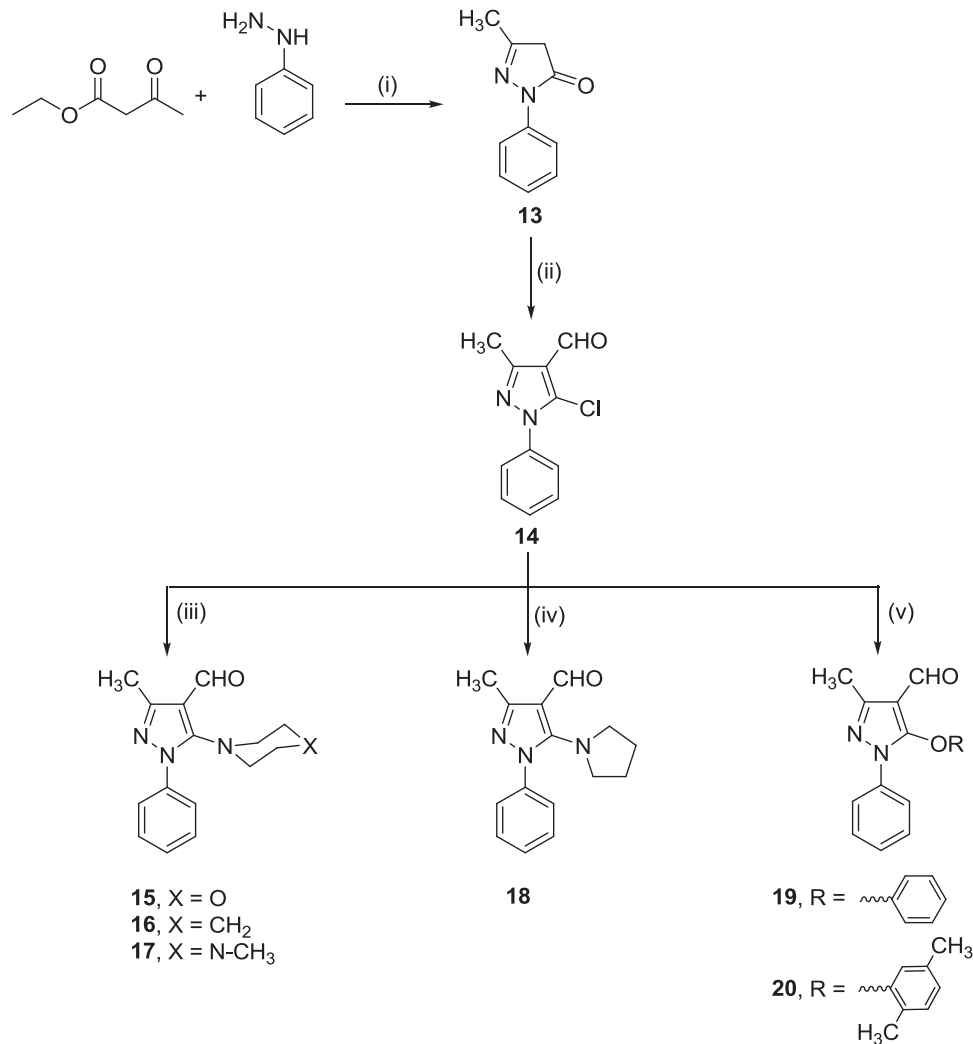
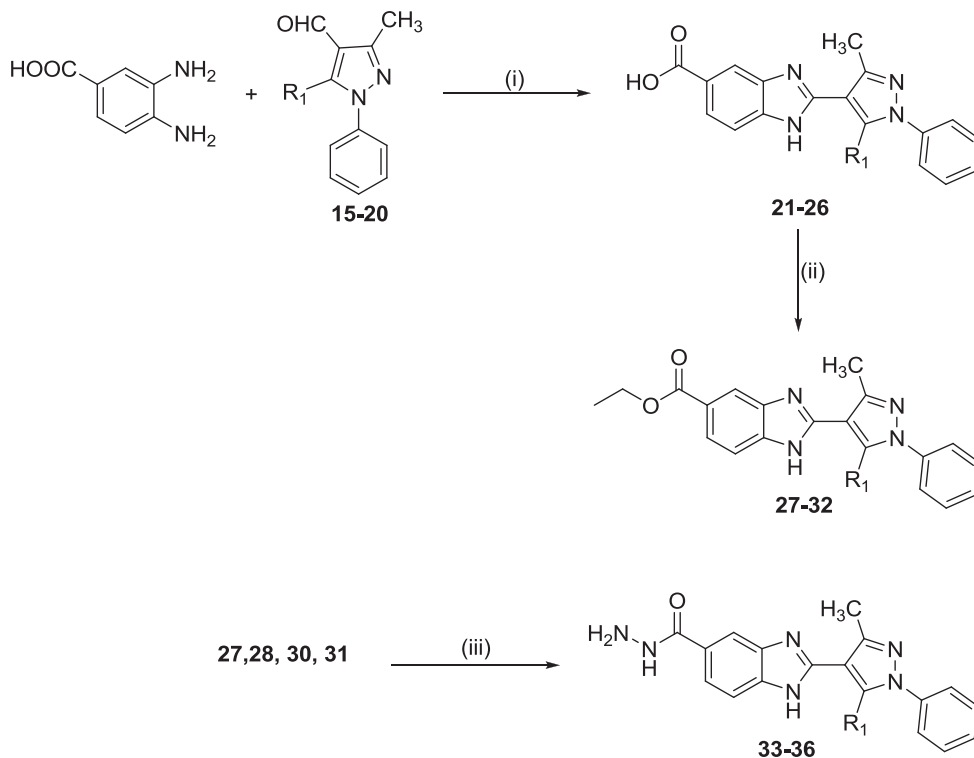


FIGURE 2 Rational design of new 5-substituted benzimidazoles as SphK1 inhibitors



SCHEME 1 Synthetic route of pyrazole-4-carboxylate derivatives **15–20**. Reagents and conditions: (i) EtOH, glacial acetic acid, reflux, 8 h; (ii) phosphorus oxychloride, dimethylformamide (DMF), reflux 2 h; (iii) morpholine, piperidine or 1-methyl piperazine, K₂CO₃ DMF, reflux 3 h; (iv) pyrrolidine, K₂CO₃ DMF, reflux 3 h; (v) phenol or 2,5-dimethylphenol, K₂CO₃ DMF, reflux 3 h



	R ₁
15, 21, 27, 33	
16, 22, 28, 34	
17, 23, 29	
18, 24, 30, 35	
19, 25, 31, 36	
20, 26, 32	

SCHEME 2 Synthetic route of compounds 21–36. Reagents and conditions: (i) 3,4-diaminobenzoic acid, Na₂S₂O₅, ethanol, stirring 6–10 h; (ii) conc. sulfuric acid, ethanol, reflux, 5–8 h; (iii) NH₂NH₂·H₂O, ethanol, reflux, 7–9 h

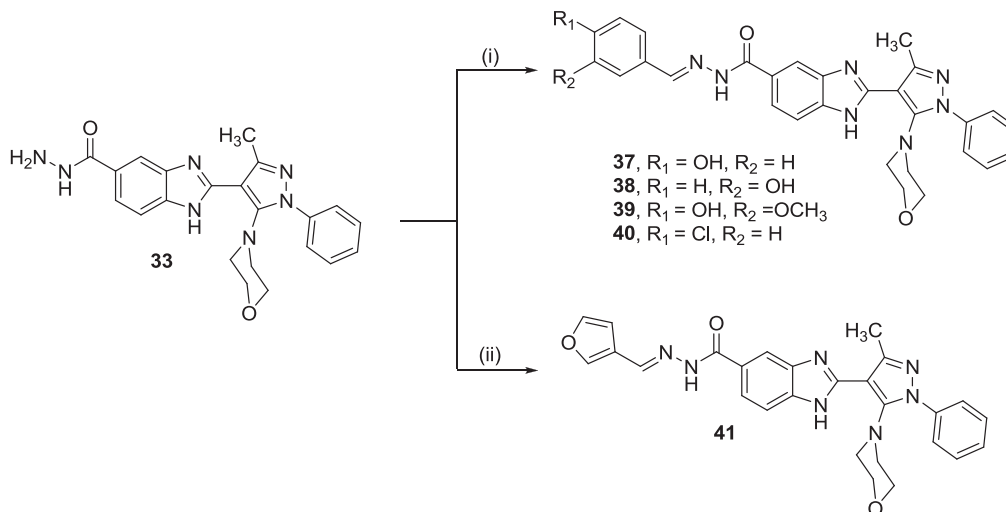
4-chlorobenzaldehyde to afford compounds 42–45, respectively (Scheme 4).

2.2 | Expression and purification of SphK1

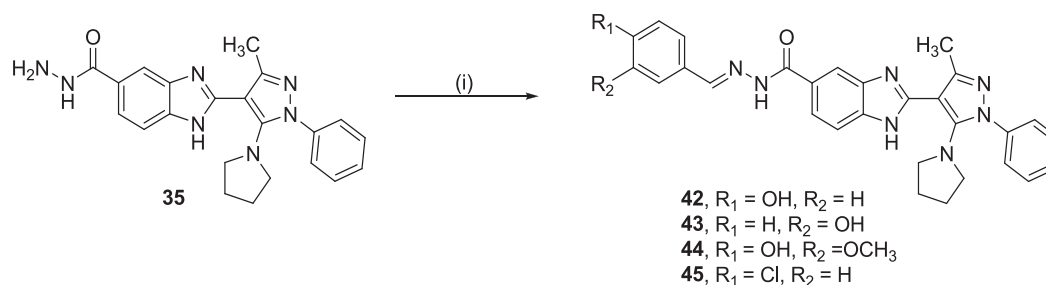
The SphK1 gene construct was cloned and expressed in BL21 Gold (DE3) cells. The inclusion bodies were solubilized with the help of *N*-lauroyl sarcosine and the solubilized protein was loaded on the Ni-NTA column and subsequently purified.^[64–67] The purified SphK1 was analyzed on sodium dodecyl sulfate–polyacrylamide gel electrophoresis (SDS-PAGE), which shows a single band of 45 kDa (Figure 3).

2.3 | Fluorescence binding studies

Fluorescence binding studies were performed to evaluate the binding affinity of all the synthesized compounds, 21–45, with SphK1. The gradual decrease in the fluorescence intensity upon addition of the selected compounds, 33, 37, 39, 41 (Figures 4a, 4c, 4e, and 4g), 42, 43, and 45 (Figures 5a, 5b, and 5c), was observed for SphK1, which suggests the formation of a stable protein–ligand complex. The rest of the compounds did not show any quenching and some of them even perturbed the structure of SphK1, as a major redshift and an increase in the fluorescence intensity were observed when they were added to protein



SCHEME 3 Synthetic route of compounds **37–41**. Reagents and conditions: (i) 4-hydroxybenzaldehyde, 3-hydroxybenzaldehyde, vanillin or 4-chlorobenzaldehyde, glacial acetic acid, ethanol, reflux, 6–8 h; (ii) furfural, glacial acetic acid, ethanol, reflux, 6–8 h



SCHEME 4 Synthetic route of compounds **42–45**. Reagents and conditions: (i) 4-hydroxybenzaldehyde, 3-hydroxybenzaldehyde, vanillin or 4-chlorobenzaldehyde, glacial acetic acid, ethanol, reflux, 6–8 h

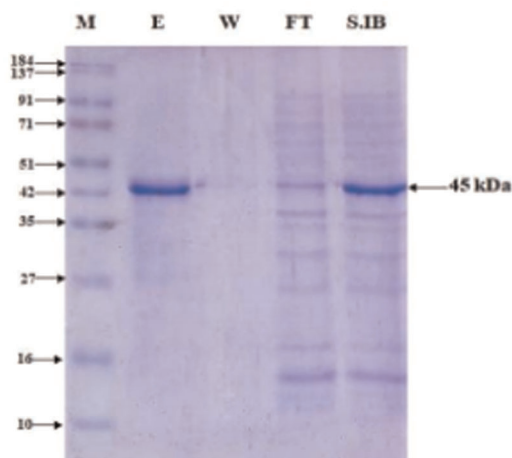


FIGURE 3 Evaluation of purity and quality of purified recombinant SphK1. Sodium dodecyl sulfate-polyacrylamide gel electrophoresis showing purified SphK1 at approximately 45 kDa. Lane 1 shows the protein ladder. Lanes 2–4 show the fractions containing purified protein after Ni-NTA chromatography

samples in increasing concentrations (data are not shown). A well-defined isosbestic point was observed at 375 nm for compound **33** interacting with SphK1, suggesting the formation of a stable protein–ligand complex. The Stern–Volmer plot (Figures 4b,d,f,h, and 5d-f) was used to analyze the quenching data to determine the binding affinity (K_a) for each compound. The number of binding sites per SphK1 molecule (n) for these compounds was also determined from the same plot. Compounds **37**, **41**, and **42** showed binding affinities in the 10^4 M range, whereas compounds **33**, **39**, **43**, and **45** showed binding in the 10^3 M range (Table 1). Thus, hits obtained from the binding studies showed a moderate binding with SphK1 and were further tested for inhibitory activity against SphK1.

2.4 | Enzyme inhibition assay

Enzyme inhibition potential against compounds **21–45** toward SphK1 was evaluated by malachite green ATPase inhibition assays. During the initial screening, the maximum concentration of all compounds ($100 \mu\text{M}$) was used (Table S2), which revealed that most

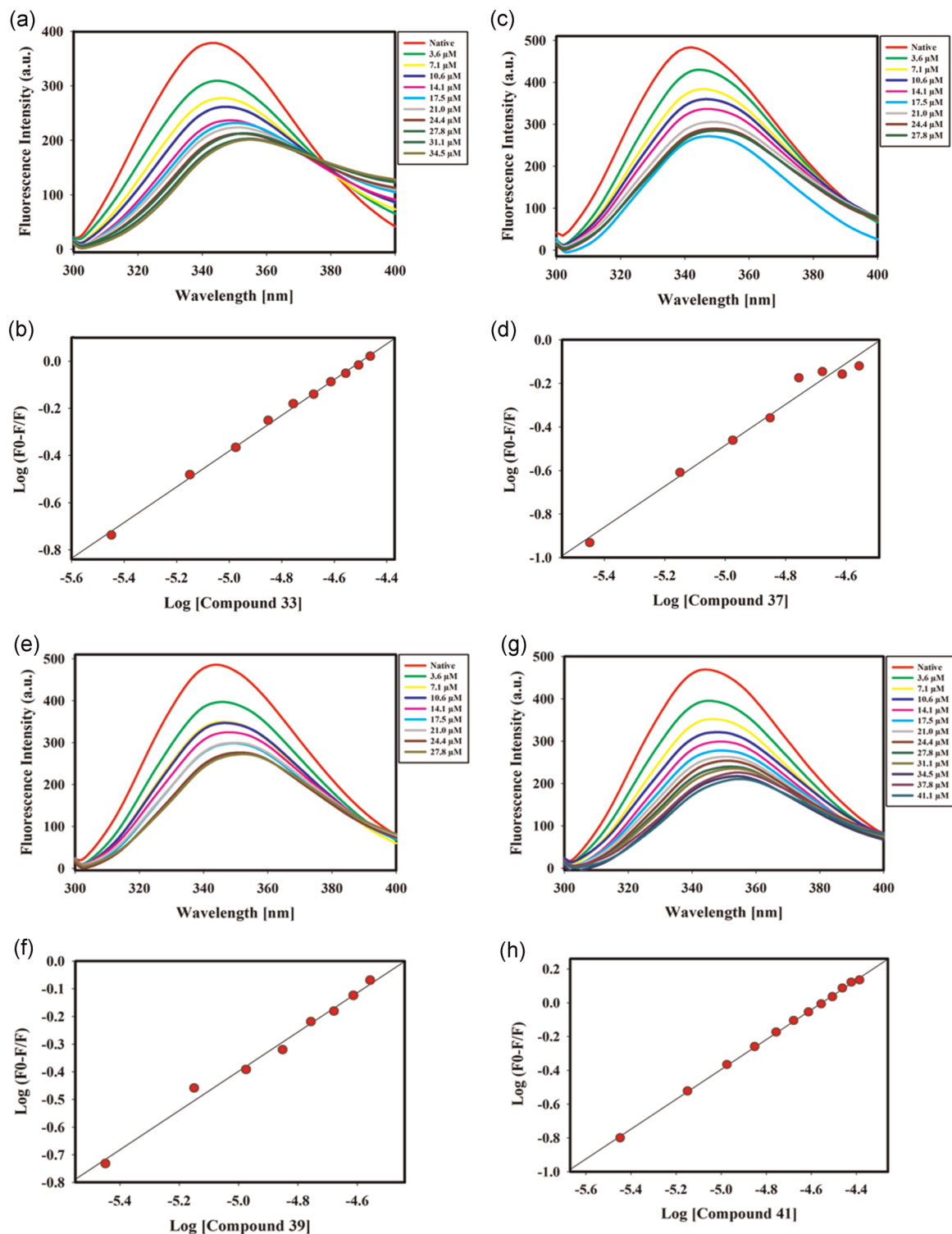


FIGURE 4 Studies of selected compounds with SphK1. Fluorescence spectra of SphK1 with increasing concentrations of (a) compounds 33 (0–34.5 mM), (c) 37 (0–27.8 mM), (e) 39 (0–27.8 mM), and (g) 41 (0–41.1 mM). Modified Stern–Volmer plot evaluating the quenching data for estimation of the binding constant (K_a) for (b) compounds 33, (d) 37, (f) 39, and (h) 41

of the studied compounds inhibited SphK1 activity effectively (Figure 6 and Table S3). The enzyme inhibitory potential of the synthesized compounds that showed good binding affinity toward the SphK1 was determined, which revealed IC_{50} values in the

micromolar range (Table 2). The kinase activity of SphK1 is measured in terms of the picomolar concentration of phosphate released in the reaction mixture, which is represented in Figures 7a–c and 8a–c. The absorbance value of the malachite-inorganic phosphate green

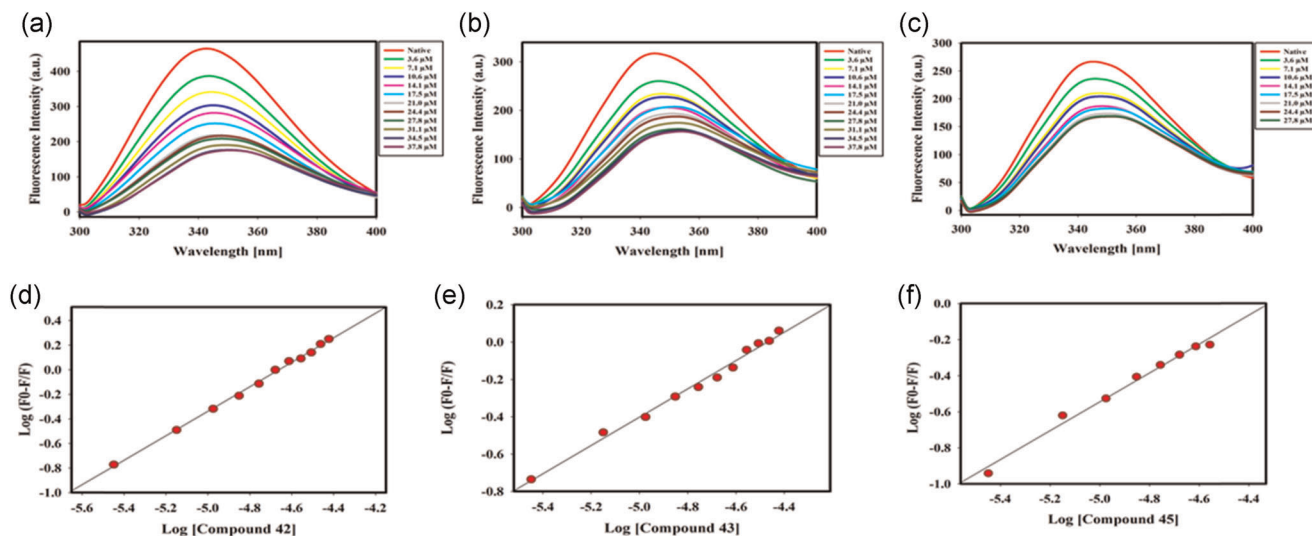


FIGURE 5 Binding studies of selected compounds with SphK1. Fluorescence spectra of SphK1 with increasing concentrations of (a) compounds 42 (0–37.8 mM), (b) 43 (0–37.8 mM), and (c) 45 (0–27.8 mM). Modified Stern–Volmer plot was used to analyze the quenching data and to estimate the binding constant (K_a) for (d) compounds 42, (e) 43, and (f) 45

TABLE 1 The binding affinity constants, number and a broad antiproliferative activity of binding sites as determined from the molecular docking and fluorescence binding experiments

Compound ID	Predicted affinity ΔG^a (kcal/mol)	b Binding affinity constant (K_a), M^{-1}	b Number of binding sites (n)
33	-8.3	2.57×10^3	0.8
37	-7.7	1.64×10^4	0.9
39	-8.0	1.41×10^3	0.7
41	-8.7	1.05×10^4	0.9
42	-8.2	4.51×10^4	1.0
43	-8.0	2.44×10^3	0.8
45	-8.8	2.82×10^3	0.8

Note: Binding parameters of the synthesized compounds with SphK1 evaluated through a molecular docking and b fluorescence binding studies.

complex so formed at 620 nm is converted with the help of the phosphate standard curve, as described.^[65-67] The loss in the SphK1 activity followed an inverse relationship between percentage inhibition and an increasing concentration of selected compounds (Figures 7d-f and 8c,d), which was used for the calculation of IC_{50} values (Table 2). Compound 41 efficiently inhibited SphK1 activity with a lowest IC_{50} value of $3.39 \pm 0.21 \mu M$ (Figure 7f). The IC_{50} value for compound 37 (Figure 7e) falls in the 4–5 μM range, whereas compounds 33 (Figure 7d), 39 (Figure 8c), 42 (Figure 8d), 43 (Figure 7e), and 45 (Figure 7d) inhibited SphK1 activity with a moderately higher IC_{50} value in the 5–7 μM range. The enzyme inhibition results overall propose that compound 41 acts as an effective inhibitor of SphK1.

2.5 | Anticancer activity against NCI-60 cell line panel

Compounds 21–45 were screened for their in vitro antiproliferative activity by the Developmental Therapeutics Program (DTP) of the National Cancer Institute (NCI) in the division of cancer treatment and diagnosis, NIH, Bethesda, MD, USA. This involves screening of the compounds at a single dose of 10 μM against a full NCI-60 cell panel including leukemia, lung, colon, brain, melanoma, ovary, kidney, prostate, and breast cancers.^[68] From the obtained results in Table 3, it is obvious that each of the screened compounds has a different degree of selectivity against 60 cell lines. K-562, MOLT-4, PRMI-8226, and SR from leukemia; SNB-75 from central nervous system cancer; UACC-62 from melanoma; A498, ACHN, CAKI-1, and UO-31 from renal cancer; PC-3 from prostate cancer; and T-47D are the most sensitive cell lines toward the tested compounds. At 10 mM concentration, compounds 33, 41, 42, 43, 44, and 45 exhibited broad antiproliferative activity against numerous cell lines (Table 3).

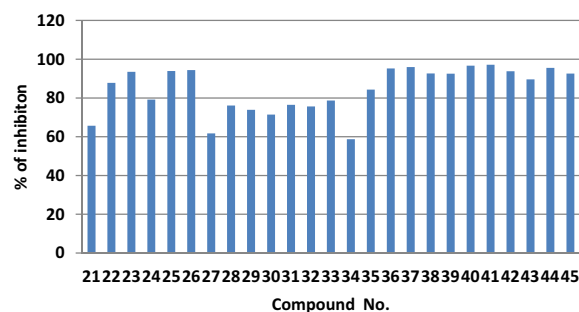


FIGURE 6 Studies of the percentage of inhibition of compounds 21–45 toward SphK1 using malachite green ATPase inhibition assays at 100 μM

TABLE 2 IC₅₀ values of the selected compounds for SphK1 inhibition calculated from the ATPase inhibition assay

Compound ID	Log IC ₅₀ (μM)	IC ₅₀ (μM)
33	0.88 ± 0.01	7.60 ± 0.25
37	0.66 ± 0.10	4.61 ± 1.04
39	0.77 ± 0.09	5.90 ± 1.19
41	0.53 ± 0.03	3.39 ± 0.21
42	0.70 ± 0.01	5.05 ± 0.13
43	0.80 ± 0.06	6.34 ± 0.86
45	0.72 ± 0.11	5.31 ± 1.28

2.6 | Molecular docking

The molecular docking study of the designed compounds with SphK1 was performed using the AutoDock Vina tool.^[69] Vina gives the predicted binding poses of the synthesized compounds 21–45 along with the binding affinities in kcal/mol. On the basis of the predicted binding affinities and interactions, compounds 33, 37, 39, 41, 42, 43, and 45 were selected as top-scoring compounds. The predicted binding affinities of the selected compounds are given in Table 4. On the basis of nonbonded interactions of compounds with the SphK1, we found that compound 41 shows comparatively better

interactions. Compound 41 shows strong bonding with SphK1 (Figure 9a–d). It forms hydrogen bonds with the residues Ser168, Asp178 (substrate-binding site), Leu268, and Gly342 (ATP-binding site) (Figure 9c). Moreover, Asp178 and Phe192 are also making π-cation bonds with the ligand. The surface view of the protein shows (Figure 9d) compound 41 to fully occupy the binding cavity. Apart from these compounds, compound 33 (Figure S26) makes a hydrogen bond with Leu299 along with π-cation interactions with the Asp178 and Phe192 of the SphK1. Compound 37 (Figure S27) forms hydrogen bonds with the Thr196, Leu268, and His311. Compound 39 (Figure S28) makes hydrogen bonds with Asp81, Asp178, Arg185, Thr196, Phe188, and Glu343. Compound 42 (Figure S29) forms hydrogen bonds with the residues Ser168, Thr196, Leu268, and Ala339. Compound 43 (Figure S30) also shows interactions with the inhibitor-binding pocket of SphK1. Compound 45 (Figure S31) also shows strong bonding with the protein by interacting with the amino acid residues Asp81, Ser168, Asp178, Thr196, Leu268, and Gly342. A detailed interaction profile of selected synthesized compounds with SphK1 is given in Tables 4 and S1.

2.7 | Structure–activity relationship

Structure–activity relationships were deduced from the foregoing results. Concerning the percentage of inhibition of the synthesized

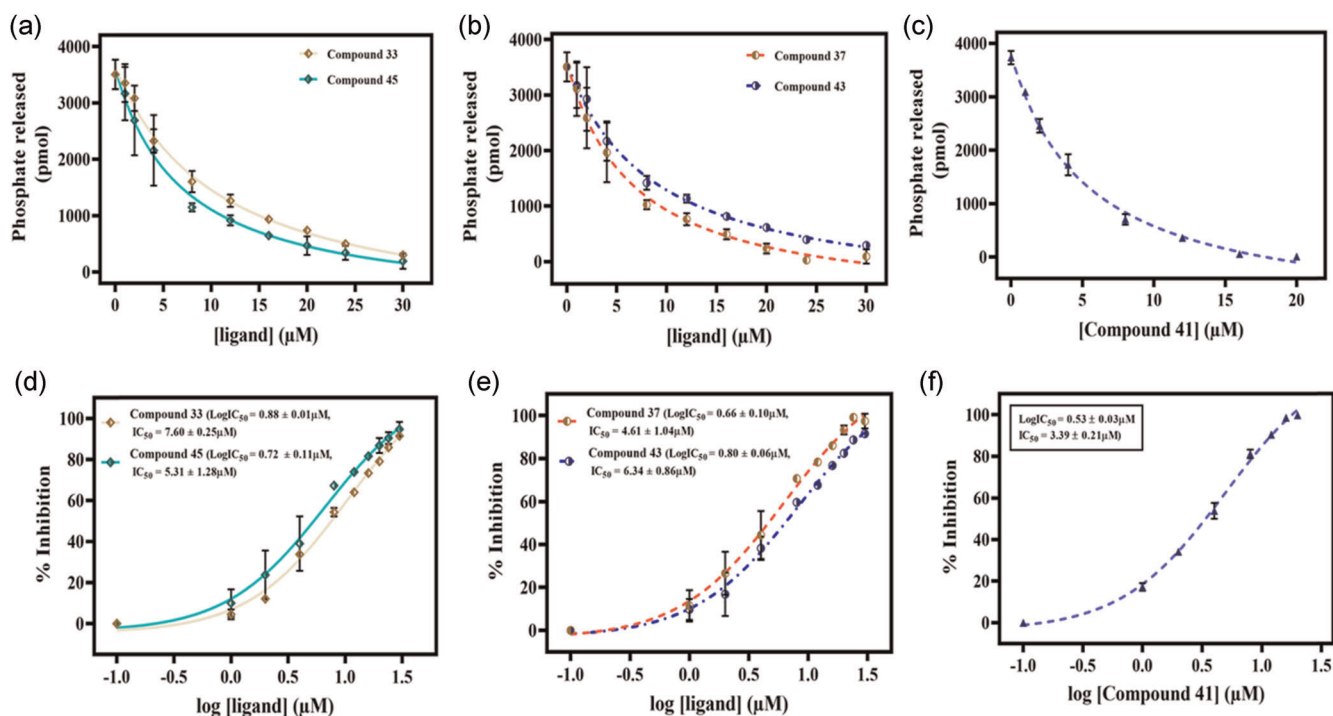


FIGURE 7 Inhibition of SphK1 ATPase activity by selected compounds. The hydrolyzed phosphate was quantified from the standard phosphate curve. The dose–response curve describing the result of increasing amount of (a) compounds 33 and 45 (0–30 μM), (b) compounds 37 and 43 (0–30 μM), and (c) compound 41 (0–20 μM) on the kinase activity of SphK1. Plots denote the percent inhibition of SphK1 activity as a function of increasing amount of (d) compounds 33 and 45, (e) compounds 37 and 43, and (f) compound 41. The IC₅₀ value was evaluated by fitting the curve from two independent experiments

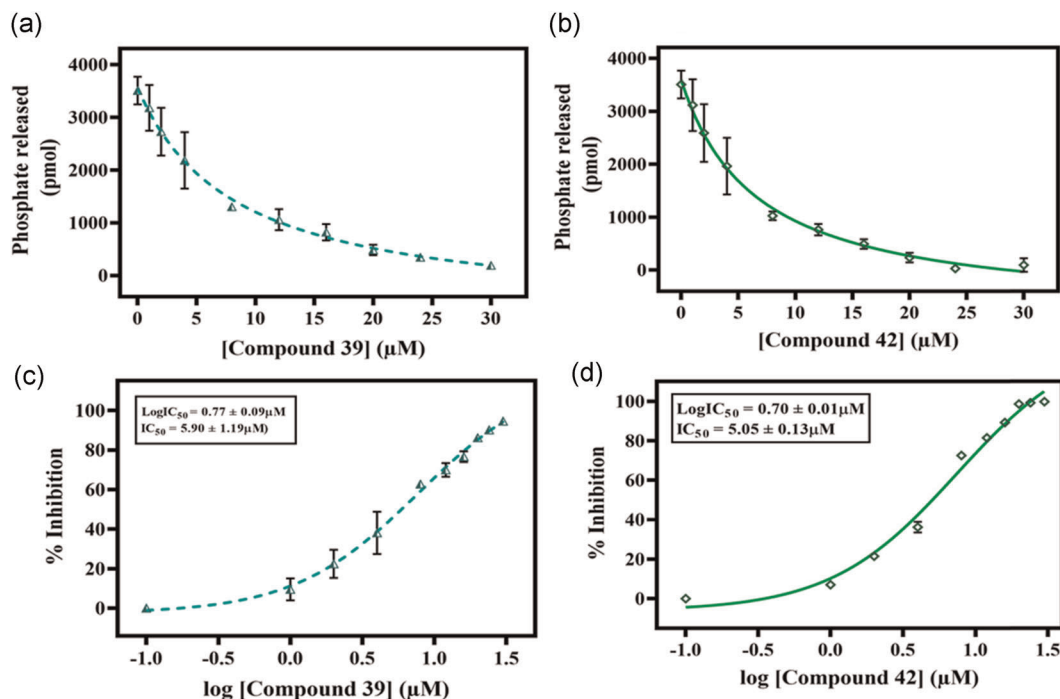


FIGURE 8 Inhibition of SphK1 activity by selected compounds. The hydrolyzed phosphate was quantified from the standard phosphate curve. The dose-response curve describing the effect of increasing amount of (a) compounds **39** and (b) **42** (0–30 μM) on the kinase activity of SphK1. Plots denote the percent inhibition of SphK1 activity as a function of increasing amount of (c) compounds **39** and (d) **42**. The IC₅₀ value was calculated by fitting the curve obtained from two independent experiments

compounds toward SphK-1, the following points can be explored. Most of the benzimidazole derivatives exert moderate to potent SphK1-inhibitory activity, and this proves the importance of polar substituents at position-5 of the benzimidazole ring. Compounds **25**, **26**, **36**, **37**, **38**, **39**, **40**, **41**, **42**, **43**, **44**, and **45** were found to be potent compounds with percentage of inhibition values 93.92%, 94.35%, 95.22%, 95.95%, 92.69%, 92.48%, 96.69%, 97.13%, 93.78%, 89.56%, 95.52%, and 92.61% (Table S2), respectively. Moreover, compounds **37**, **38**, **39**, **40**, **41**, **42**, **43**, **44**, and **45**, with azomethine group, exhibited potent inhibitory activity toward SphK-1 acetohydrazide derivatives **33** and **35**. It is worth mentioning that these results were correlated with our main rationale that aimed to elongate the acetohydrazide chain by adding azomethine group. In addition, attaching the azomethine group with a five-membered ring, like compound **41**, instead of the phenyl ring in compounds **37**, **38**, **39**, **40**, **42**, **43**, **44**, and **45** improves the inhibitory activity. Comparing the inhibitory activity of these compounds with the IC₅₀ values and cytotoxicity, it is clear that there is a correlation between the results and our rationale. The IC₅₀ values of compounds **33**, **37**, **39**, **41**, **42**, **43**, and **45** showed the importance of substituting 5-position of the benzimidazole ring with polar groups, as the COOH and the amino group of the carbohydrazide are essential for activity. These data are consistent with our rationale, which depends on replacing the hydroxyl group of the polar end to prevent its phosphorylation by other polar groups, and this was of great importance in the design of novel sphingosine-based SKIs. Modification of the polar head to possess the groups R₁ = COOH, ester, CONHNH₂, CONHN=CH-C₆H₄OH was planned,

so that carboxylic group, the amino group of the carbohydrazide and of the hydrazide moiety, and the phenolic OH of the 4-hydroxyphenyl group will be the polar heads.

The inhibitory effect of the carbohydrazide derivatives **37**, **39**, **41**, **42**, and **45** (IC₅₀ = 4.61 ± 1.04, 5.90 ± 1.19, 3.39 ± 0.21, 5.05 ± 0.13 and 5.31 ± 1.28 μM, respectively), with CONHN=CH-group in 5-position, is higher than the hydrazide derivative (CONHNH₂), **33** (IC₅₀ = 7.60 ± 0.25 μM). These data also are correlated with our rationale, which depends on structure elongation on the carbohydrazide (CONHNH₂) to CONHN=CH-. In addition, substituting with hydrazine at 5-position of the benzimidazole ring decreased the binding affinity. Comparing the inhibitory effect of compound **41** (IC₅₀ = 3.39 ± 0.21 μM) with the other hydrazide derivatives **37**, **39**, **42**, and **45** (IC₅₀ = 4.61 ± 1.04, 5.90 ± 1.19, 5.05 ± 0.13, and 5.31 ± 1.28 μM, respectively), it was observed that attaching the CH=N group with a five-membered ring instead of phenyl ring enhanced the inhibitory effect and the binding affinity. Also, it was observed that substitution with methoxy group in the phenyl ring decreased the inhibitory effect of compound **39** (IC₅₀ = 5.90 ± 1.19 μM), compared with the unsubstituted **37** (IC₅₀ = 4.61 ± 1.04 μM). Compound **37** (IC₅₀ = 4.61 ± 1.04 μM) with morpholine substituent on the pyrazole ring exhibited a higher inhibitory effect than compound **42** (IC₅₀ = 5.05 ± 0.13 μM) with pyrrole substituent on the pyrazole ring. Comparing the effect of the ester group at 5-position of the benzimidazole ring in compound **23** (IC₅₀ = 6.34 ± 0.86) with that of the hydrazide group in compound **33** (IC₅₀ = 7.60 ± 0.25), it was deduced that the presence of an ester group was more favorable

TABLE 3 In vitro growth inhibition % (GI %) of some synthesized benzimidazole derivatives against a panel of tumor cell lines at 10 μM

Subpanel	21	22	23	24	25	26	27	28	29	30	31	32	33	34	35	36	37	38	39	40	41	42	43	44	45	
Leukemia																										
CCRF-CEM	-	-	-	-	-	-	-	-	-	-	-	-	56	-	-	11	58	-	52	28	51	41	49	49	40	
HL-60(TB)	-	-	-	-	-	-	-	-	-	-	-	-	47	23	21	-	59	-	20	25	52	28	58	47	39	
K-562	-	15	-	16	22	28	-	-	-	-	23	-	33	11	19	-	53	10	25	19	49	57	53	43	60	
MOLT-4	-	-	-	18	17	27	-	-	-	13	25	-	35	14	26	15	65	13	-	28	44	40	54	37	52	
PRMI-8226	-	10	-	18	19	23	-	-	14	-	19	14	50	-	18	15	50	23	12	12	67	49	49	34	65	
SR	-	14	26	19	24	38	-	20	-	25	26	-	68	12	21	26	50	16	11	15	52	79	47	47	54	
Non-small-cell lung cancer																										
A549/ATTC	-	-	-	12	-	19	-	-	-	-	-	-	49	-	11	-	60	-	29	11	61	69	47	57	62	
EKVX	-	-	-	-	19	-	-	-	-	-	-	-	48	-	-	12	63	-	-	37	45	-	43	59	39	
HOP-62	14	12	-	-	13	12	10	-	-	10	10	52	-	-	14	58	-	18	20	47	74	37	26	58		
HOP-92	10	10	-	-	-	14	13	-	-	10	-	60	-	-	20	54	-	10	34	49	57	39	65	41		
NCI-H226	15	-	-	-	-	-	-	-	-	12	-	-	64	-	-	26	56	-	21	45	33	44	38	45	50	
NCI-H23	19	18	11	-	-	-	-	-	-	-	-	-	61	-	-	-	64	-	20	28	51	50	44	42	45	
NCI-H322M	-	-	-	-	14	24	-	-	10	-	-	-	53	-	-	-	54	-	-	27	39	50	40	54	56	
NCI-H460	-	-	-	-	-	13	-	-	-	-	-	-	49	-	-	-	53	-	-	38	57	48	39	76	58	
NCI-H522	-	-	-	-	13	nd	10	-	-	-	-	-	48	19	16	12	54	19	23	15	47	32	38	63	24	
Colon cancer																										
COLO 205	-	-	-	-	-	-	-	-	-	-	-	-	47	-	-	-	55	-	-	23	49	52	43	59	34	
HCC-2998	-	-	-	-	-	-	-	-	-	-	-	-	46	-	-	-	55	-	-	25	38	64	45	58	45	
HCT-116	10	17	-	19	26	33	-	-	-	-	19	-	43	-	15	-	58	-	12	28	40	56	47	58	27	
HCT-15	-	-	-	-	11	11	-	-	-	-	-	-	42	-	18	-	57	-	23	28	51	45	40	69	24	
HT29	-	-	-	-	-	nd	-	-	-	-	-	-	43	-	-	-	59	-	13	27	52	-	39	70	17	
KM12	-	-	-	-	-	14	-	-	-	-	-	-	44	-	12	-	58	-	12	28	59	67	53	46	26	
SW-620	-	-	-	-	-	-	-	-	-	-	-	-	45	-	-	-	59	-	26	26	39	50	58	64	39	
CNS cancer																										
SF-268	-	-	-	-	11	10	-	-	12	-	-	-	46	10	-	-	54	-	21	27	51	34	13	54	22	
SF-295	-	-	-	-	-	-	-	-	-	-	-	-	47	-	-	-	53	-	18	30	45	56	60	45	16	
SF-539	-	-	-	-	-	-	-	-	-	-	-	-	51	-	-	-	56	-	32	33	53	78	63	67	37	
SNB-19	-	-	-	-	-	-	-	-	-	-	-	-	52	-	-	-	54	-	-	32	65	59	64	78	39	
SNB-75	20	16	-	14	14	12	15	18	-	13	-	-	51	-	-	15	44	17	13	11	54	63	19	63	50	
U251	14	11	-	-	-	10	-	-	-	-	-	-	52	-	-	11	44	-	27	32	67	69	58	62	30	
Melanoma																										
LOX IMVI	-	11	-	11	15	11	-	-	12	-	10	-	55	-	18	17	59	-	-	23	62	71	60	53	69	
MALME-3M	11	-	19	-	-	13	-	-	-	-	-	-	56	-	-	-	58	-	-	28	54	69	49	57	67	
M14	-	-	-	11	-	-	-	10	-	-	-	-	57	-	-	-	49	-	-	29	54	54	42	60	69	
MDA-MB-435	-	-	21	-	-	-	-	-	-	-	-	-	40	-	12	-	60	-	12	29	49	74	50	66	49	
SK-MEL-2	-	-	-	nd	-	-	-	-	-	-	-	-	30	-	-	nd	59	-	-	29	48	78	39	57	39	
SK-MEL-28	-	-	-	-	-	-	-	-	-	-	-	-	60	-	-	-	58	-	45	31	57	81	39	49	65	
SK-MEL-5	-	-	-	-	-	-	-	-	-	-	-	-	49	-	-	-	58	-	-	31	59	58	39	68	75	
UACC-257	-	-	-	-	-	-	-	-	-	-	-	-	49	-	-	-	58	-	-	29	49	80	43	39	64	
UACC-62	-	28	15	23	23	43	11	10	21	14	30	19	50	16	37	22	57	14	21	33	50	74	43	59	32	
Ovarian cancer																										
IGROV1	13	20	-	31	33	51	-	-	-	-	26	15	55	-	17	18	49	-	-	18	58	40	43	59	31	
OVCAR-3	19	10	-	11	13	23	-	-	-	-	-	-	53	-	-	-	48	-	12	12	56	50	50	20	33	
OVCAR-4	-	13	-	13	16	21	-	-	-	-	14	-	54	-	18	12	49	-	12	13	61	59	45	16	38	
OVCAR-5	-	29	-	-	-	16	-	-	-	-	-	-	55	-	-	-	68	-	13	14	62	64	53	45	36	
OVCAR-8	-	-	-	-	11	12	-	-	-	-	-	-	59	-	-	-	48	-	14	15	63	61	49	55	44	
NCI/ADR-RES	-	10	-	-	-	10	-	-	-	-	10	-	58	-	10	-	59	-	21	29	67	52	53	68	11	
SK-OV-3	-	-	-	-	11	14	-	-	-	-	12	-	59	-	-	-	52	-	11	28	48	59	52	69	45	

(Continues)

TABLE 3 (Continued)

Subpanel	21	22	23	24	25	26	27	28	29	30	31	32	33	34	35	36	37	38	39	40	41	42	43	44	45
Renal cancer																									
786-0	-	-	-	-	-	12	-	-	-	-	-	-	50	-	-	-	53	-	11	30	59	59	52	68	56
A498	29	44	30	35	45	48	-	21	29	30	39	32	52	23	46	29	21	-	14	33	54	59	55	55	43
ACHN	13	10	-	-	10	14	-	-	-	10	14	-	51	-	11	13	53	11	15	31	65	65	52	45	52
CAKI-1	24	29	21	40	35	58	18	20	23	17	33	14	43	20	27	21	21	16	10	23	56	38	54	45	67
RXF 393	-	-	-	-	-	-	-	-	-	-	-	-	42	-	-	-	32	-	12	25	62	32	23	53	56
SN 12C	-	-	-	-	-	-	-	-	-	-	-	-	43	-	-	-	33	-	32	29	53	36	39	47	34
TK-10	-	-	-	-	-	nd	-	-	-	-	-	-	45	-	-	-	34	-	25	27	56	34	11	62	62
UO-31	30	29	24	33	38	37	21	13	30	25	24	29	46	18	27	30	29	15	18	21	44	29	31	50	52
Prostate cancer																									
PC-3	13	17	-	18	17	23	10	-	13	-	19	14	44	-	24	13	30	15	31	31	59	36	35	51	49
DU-145	-	-	-	-	-	-	-	-	-	-	-	-	41	-	-	-	32	-	17	33	58	14	13	45	46

Abbreviations: -, growth inhibition % produced by the compound is below 10%; nd, not determined.

for the activity. Reacting compound **33** with different aldehydes to form a carbonylhydrazone with CH=N group and increasing the chain in 5-position of the benzimidazole ring were found to be essential for activity.

3 | CONCLUSION

In search of effective SphK1 inhibitors, a new series of benzimidazole derivatives **21–45** was rationally designed and synthesized bearing pyrazole derivatives at 2-position and polar groups at 5-position. We have observed that seven compounds possessing different scaffolds showed excellent binding affinity and inhibitory potential toward SphK1. All these molecules form a significant number of hydrogen bonds and van der Waals interactions with the catalytic site residues. The novel scaffolds would be implicated in cancer therapy after the required in vivo validation.

Compounds **33**, **37**, **39**, **41**, **42**, **43**, and **45** showed an effective binding affinity toward SphK1 and significantly inhibited SphK1. Also, the synthesized compounds were evaluated by the NCI DPT for testing their antiproliferative activity on a panel of 60 cell lines, and compounds **33**, **41**, **42**, **43**, and **45** exhibited broad antiproliferative activity on a wide spectrum of cancer cell lines. The results showed that compound **41** was most potent with an IC₅₀ value of 3.39 ± 0.21 μM and a broad antiproliferative activity against numerous cell lines. Molecular docking studies of the synthesized compounds in the SphK1 enzyme displayed their ability to form important hydrogen bonding interactions. Also, compound **41** showed a high binding affinity toward SphK1 enzyme. A significant correlation between the cytotoxic activity, molecular docking, and enzyme inhibition results is clear to give insight into the importance of these benzimidazoles as potent SphK1 inhibitors, which could be further implicated in the

therapeutic management of cancer and other SphK1-associated diseases.

4 | EXPERIMENTAL

4.1 | General

Luria broth and Luria agar were purchased from Himedia. Plasmid pET28b+, DH5α, and BL21-Gold cells were procured from Invitrogen. Ni-NTA column was purchased from GE Healthcare Life Sciences. *N*-Lauroyl sarcosine, Tris buffer, dimethyl sulfoxide (DMSO), and other reagents were purchased from Sigma-Aldrich. BIOMOL® was obtained from Enzo. All the reagents used for buffer and chemical preparation were of analytical grade. Microanalyses and spectral data of the compounds were performed in the Microanalytical Center at National Research Centre and Pharmaceutical Faculty, Cairo University, Egypt, and Helmholtz Institute for Pharmaceutical Research Saarland (HIPS)–Helmholtz Centre for Infection Research (HZI), Saarbrücken, Germany. The IR spectra (4000–400 cm⁻¹) were recorded using KBr pellets in a Jasco FT/IR 300E Fourier transform infrared spectrophotometer on a PerkinElmer FT-IR 1650 spectrophotometer. The ¹H nuclear magnetic resonance (NMR) spectra (see the Supporting Information) were recorded using 500 and 400 MHz NMR spectrometer. Chemical shifts are reported in parts per million (ppm) from the tetramethylsilane resonance in the indicated solvent. Coupling constants (*J*) are reported in Hertz (Hz), and integration (where applicable); spectral splitting patterns are designed as follows: singlet (s); doublet (d); triplet (t); quartet (q); multiplet (m); and broad singlet (brs). The samples were referenced to the appropriate internal nondeuterated solvent peak. The data are given as follows: chemical shift (δ) in ppm, multiplicity (where applicable). The mass spectra were recorded

TABLE 4 Interaction profile of compounds 33, 37, 39, 41, 42, 43, and 45 with SphK1

Compound ID	Interaction type	No. of interactions	Interacting residues
33	van der Waals	9	Phe173, Thr196, Leu259, Leu261, Met272, Ala274, Phe288, Leu299, His311
	Hydrogen bond	1	Leu299
	π -Cation	2	Asp178, Phe192
	π -Sigma	3	Ile174, Leu302, Phe303
	π -Sulfur	1	Met306
	π -Alkyl	4	Val177, Leu268, Val290, Leu319
37	van der Waals	11	Leu169, Phe173, Leu259, Gly269, Leu261, Ala274, Leu299, His311, Val340, Asp341, Gly342
	Hydrogen bond	3	Thr196, Leu268, His311
	π -Cation/anion	4	Asp178, Phe192, Met272, Met306
	π -Alkyl	6	Ala170, Ile174, Val177, Val290, Leu319, Ala339
	π -Sigma	1	Leu302
	π - π Stacked	1	Phe303
39	van der Waals	18	Leu167, Ser168, Ala170, Phe173, Val177, Glu189, Leu259, Leu261, Gly269, Ala274, Leu299, Leu302, Phe303, Met306, His311, Ala339, Asp341, Gly342
	Hydrogen bond	6	Asp81, Asp178, Arg185, Thr196, Phe188, Glu343
	π -Anion	1	Asp81
	π -Alkyl	6	Ala115, Ile174, Phe192, Leu268, Met272, Leu319
	π -Sulfur	1	Met272
41	van der Waals	10	Ala115, Ser168, Thr196, Leu261, Leu259, Gly269, Ala274, Leu299, His311, Gly342
	Hydrogen bond	4	Ser168, Asp178, Leu268, Gly342
	π -Cation/anion	2	Asp178, Phe192
	π -Sigma	3	Ile174, Leu302, Phe303
	π -Alkyl	6	Ala170, Phe173, Val177, Val290, Leu319, Ala339
	π -Sulfur	2	Met272, Met306
42	van der Waals	8	Leu169, Leu261, Gly269, Ala274, His311, Val340, Asp341, Gly342
	Hydrogen bond	4	Ser168, Thr196, Leu268, Ala339
	π -Sigma	1	Leu302
	π -Cation/anion	3	Asp178(2), Phe192
	π -Alkyl	13	Phe173, Ile174(2), Ala170, Val177, Leu259, Leu268, Val290, Leu299, Phe303, Met306, Leu319, Ala339
	π - π Stacked	2	Phe192, Phe303
	π -Sulfur	1	Met272
43	van der Waals	10	Ala115, Leu169, Leu261, Gly269, Ala274, Leu299, His311, Val340, Asp341, Glu343
	Hydrogen bond	5	Ser168, Thr196, Leu268, Ala339, Gly342
	π -Cation/anion	2	Asp178, Phe192
	π -Alkyl	9	Ala170, Phe173, Ile174, Val177, Leu259, Leu268, Val290, Leu319, Ala339
	π -Sigma	2	Ile174, Leu302
	π - π Stacked	2	Phe192, Phe303
	π -Sulfur	2	Met272, Met306
45	van der Waals	15	Gly26, Gly80, Gly80, Ser112, Gly113, Asn114, Ala170, Arg185, Glu189, Thr196, Leu261, Gly269, Ala339, Asp341, Glu343
	Hydrogen bond	6	Asp81, Ser168, Asp178, Thr196, Leu268, Gly342
	π -Cation/anion	3	Asp81, Asp178, Arg191
	π -Alkyl	7	Ala115(2), Ile174, Leu167, Val177, Leu268, Met272
	π - π Stacked	1	Phe192
	π -Sulfur	1	Met272

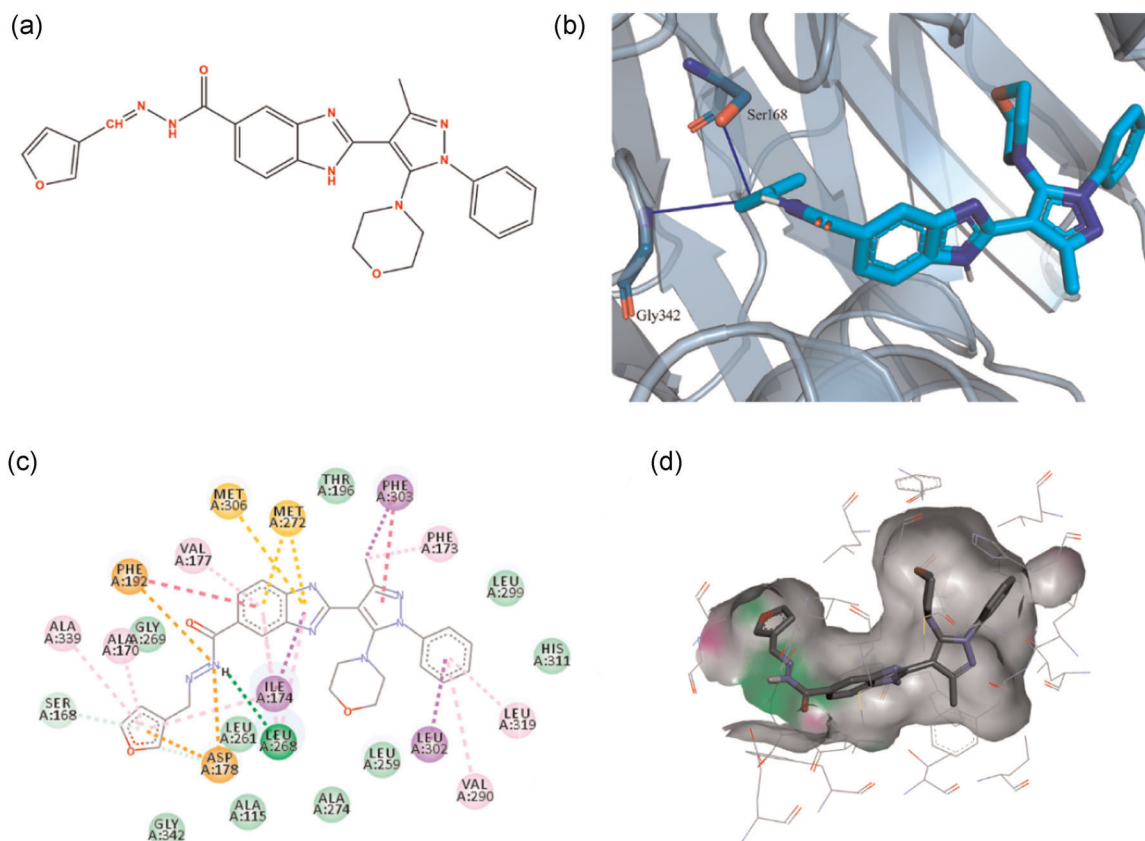


FIGURE 9 Docked pose of compound **41** with the SphK1. (a) Chemical structure of compound **41**. (b) Graphical representation of compound **41** interacting with binding site residues of SphK1. (c) Two-dimensional scheme of protein-ligand interactions. (d) Surface view of SphK1 binding pocket occupied by compound **41**

using a Finnigan mat SSQ 7000 (Thermo Instrument Systems Inc.) spectrometer at 70 eV. Chromatography solvents were of high-performance liquid chromatography grade and were used without further purification. Thin-layer chromatography (TLC) analysis was performed using Merck silica gel 60 F-254 thin-layer plates. Starting materials, reagents, and solvents for reactions were of reagent grade and used as purchased. The petroleum ether had a boiling temperature in the 60–80°C range.

The InChI codes of the investigated compounds, together with some biological activity data, are provided as Supporting Information.

4.2 | Chemistry

4.2.1 | General procedure for the synthesis of compounds **21–26**

A suspension of 3,4-diaminobenzoic acid (9.2 mmol) and sodium metabisulfite (7 g, 36.8 mmol) dissolved in absolute ethanol (40 ml) was added to a solution of different pyrazole derivatives **15–20**^[61–63] (9.2 mmol) dissolved in absolute ethanol (30 ml). The mixture was stirred for 6–10 h and monitored by TLC. The reaction mixture was poured on crushed ice; the resulting precipitate was

collected by filtration, dried, and recrystallized from ethanol to give compounds **21–26**.

2-(3-Methyl-5-morpholino-1-phenyl-1H-pyrazol-4-yl)-1H-benzo[d]imidazole-5-carboxylic acid (21)

Yield = 73.5%; mp: 192–194°C; R_f = 0.23 (petroleum ether/EtOAc = 1:3.5); IR (KBr): $\nu_{\max}/\text{cm}^{-1}$: 3423 (NH), 3097 (CH aromatic), 2966 (CH aliphatic), 2855 (OH), 1627 (C=N), 1590 (C=C), 1693 (C=O); ^1H NMR (DMSO- d_6 , 400 MHz): δ_{H} 2.29 (s, 3H, CH₃), 2.93 (s, 4H, H3, H5 morpholine protons), 3.50 (s, 4H, H2, H6 morpholine protons), 7.39–7.43 (m, 1H, aromatic proton), 7.52–7.56 (m, 2H, aromatic protons), 7.65–7.73 (m, 3H, aromatic protons), 7.85 (d, J = 7.2 Hz, 1H, aromatic proton), 8.21 (s, 1H, aromatic proton), 12.63 (brs, 1H); ^{13}C NMR (DMSO- d_6 , 125 MHz): δ_{C} 13.29, 49.97, 65.94, 103.75, 123.39, 124.23, 127.47, 129.02, 139.09, 147.49, 148.90, 167.88; mass spectrometry (MS) (electrospray ionization [EI], 70 eV): m/z (%) 404.0 (100) $[\text{M}]^+$, 405.2 (40) $[\text{M}+1]^+$. Anal. calcd. for C₂₂H₂₁N₅O₃ (FW: 404): C, 65.50; H, 5.25; N, 17.36. Found: C, 65.65; H, 5.42; N, 17.47.

2-[3-Methyl-1-phenyl-5-(piperidin-1-yl)-1H-pyrazol-4-yl]-1H-benzo[d]imidazole-5-carboxylic acid (22)

Yield = 80.5%; mp: 156–158°C; R_f = 0.18 (petroleum ether/EtOAc = 1:4); IR (KBr): $\nu_{\max}/\text{cm}^{-1}$: 3427 (NH), 3088 (CH aromatic), 2924 (CH aliphatic), 1833 (C=O), 1626 (C=N), 1596 (C=C); ^1H NMR (DMSO-

d_6 , 400 MHz): δ_H 1.36–1.37 (m, 6H, H3, H4, H5 piperidine protons), 2.23 (s, 3H, CH₃), 2.83–2.84 (m, 4H, H2, H6 piperidine protons), 7.36–7.40 (m, 1H, aromatic proton), 7.50–7.54 (m, 2H, aromatic protons), 7.65–7.70 (m, 3H, aromatic protons), 7.84 (d, $J = 8.0$ Hz, 1H, aromatic protons), 8.21 (s, 1H, aromatic proton), 12.69 (brs, 1H); ¹³C NMR (DMSO- d_6 , 125 MHz): δ_C 13.24, 23.33, 25.18, 50.96, 102.97, 123.92, 127.21, 128.97, 139.45, 147.45, 150.12, 167.91; MS (EI, 70 eV): m/z (%) 402.2 (100) [M+1]⁺, 403.2 (25) [M+2]⁺. Anal. calcd. for C₂₃H₂₃N₅O₂ (FW: 401): C, 68.81; H, 5.77; N, 17.44. Found: C, 68.95; H, 5.76; N, 17.59.

2-[3-Methyl-5-(4-methylpiperazin-1-yl)-1-phenyl-1H-pyrazol-4-yl]-1H-benzo[d]imidazole-5-carboxylic acid (23)

Yield = 42%; mp: 289–291°C; $R_f = 0.53$ (EtOAc/methanol = 1:1); IR (KBr): $\nu_{\max}/\text{cm}^{-1}$: 3439 (NH), 3066 (CH aromatic), 2962 (CH aliphatic), 1689 (C=O), 1625 (C=C), 1594 (C=C); ¹H NMR (DMSO- d_6 , 500 MHz): δ_H 2.11 (s, 3H, CH₃), 2.24–2.25 (m, 7H, CH₃ + 4H piperazine protons), 2.91–2.93 (m, 4H, piperazine protons), 7.37–7.40 (m, 1H, aromatic proton), 7.50–7.53 (m, 2H, aromatic protons), 7.64 (d, $J = 8.5$ Hz, 1H, aromatic proton), 7.69 (d, $J = 7.5$ Hz, 2H, aromatic proton), 7.84 (d, $J = 8.5$ Hz, 1H, aromatic proton), 8.20 (s, 1H, aromatic proton), 12.63 (brs, 1H); ¹³C NMR (DMSO- d_6 , 125 MHz): δ_C 13.65, 40.00, 48.61, 53.96, 103.72, 125.09, 128.92, 130.34, 139.43, 147.97, 148.98, 149.20, 170.91; MS (EI, 70 eV): m/z (%) 417.2 (50) [M+1]⁺. Anal. calcd. for C₂₃H₂₄N₆O₂ (FW: 416): C, 66.33; H, 5.81; N, 20.18. Found: C, 66.49; H, 5.72; N, 20.27.

2-(3-Methyl-1-phenyl-5-(pyrrolidin-1-yl)-1H-pyrazol-4-yl)-1H-benzo[d]imidazole-5-carboxylic acid (24)

Yield = 51.4%; mp: 169–171°C; $R_f = 0.25$ (petroleum ether/EtOAc/ethanol = 1:2:0.5); IR (KBr): $\nu_{\max}/\text{cm}^{-1}$: 3423 (NH), 3060 (CH aromatic), 2927 (CH aliphatic), 1695 (C=O), 1624 (C=N), 1542 (C=C); ¹H NMR (DMSO- d_6 , 500 MHz): δ_H 1.70–1.73 (m, 4H, H3, H4 pyrrolidine protons), 2.23 (s, 3H, CH₃), 2.95–2.98 (m, 4H, H2, H5 pyrrolidine protons), 7.38–7.41 (m, 1H, aromatic proton), 7.49–7.52 (m, 2H, aromatic protons), 7.56 (d, $J = 7.0$ Hz, 2H, aromatic protons), 7.62 (d, $J = 8.5$ Hz, 1H, aromatic protons), 7.82 (dd, 1H, $J = 8.5$ Hz, $J = 1.5$ Hz, aromatic proton), 8.16 (s, 1H, aromatic proton), 12.60 (brs, 1H); ¹³C NMR (DMSO- d_6 , 125 MHz): δ_C 13.32, 25.28, 51.12, 100.49, 125.10, 127.37, 129.10, 141.04, 147.54, 168.22; MS (EI, 70 eV): m/z (%) 388.1 (100) [M+1]⁺, 389.2 (27) [M+2]⁺. Anal. calcd. for C₂₂H₂₁N₅O₂ (FW: 387): C, 68.20; H, 5.46; N, 18.08. Found: C, 68.35; H, 5.65; N, 18.26.

2-(3-Methyl-5-phenoxy-1-phenyl-1H-pyrazol-4-yl)-1H-benzo[d]imidazole-5-carboxylic acid (25)

Yield = 75%; mp: 138–140°C; $R_f = 0.53$ (petroleum ether/EtOAc/ethanol 1:2:0.25); IR (KBr): $\nu_{\max}/\text{cm}^{-1}$: 3435 (NH), 3066 (CH aromatic), 2927 (CH aliphatic), 1690 (C=O), 1629 (C=N), 1594 (C=C); ¹H NMR (DMSO- d_6 , 400 MHz): δ_H 2.62 (s, 3H, CH₃), 6.95–6.96 (m, 3H, aromatic protons), 7.19–7.24 (m, 2H, aromatic protons), 7.33–7.37 (m, 1H, aromatic proton), 7.45–7.49 (m, 3H, aromatic protons), 7.65–7.68 (m, 2H, aromatic protons), 7.75 (s, 1H, aromatic

protons), 8.17 (s, 1H, aromatic proton), 12.37 (s, 1H); MS (EI, 70 eV): m/z (%) 411.1 (100) [M+1]⁺, 412.2 (25) [M+2]⁺. Anal. calcd. for C₂₄H₁₈N₄O₃ (FW: 410): C, 70.23; H, 4.42; N, 13.65. Found: C, 70.33; H, 4.35; N, 13.71.

2-[5-(2,5-Dimethylphenoxy)-3-methyl-1-phenyl-1H-pyrazol-4-yl]-1H-benzo[d]imidazole-5-carboxylic acid (26)

Yield = 37%; mp 153–155°C; $R_f = 0.53$ (petroleum ether/EtOAc/methanol = 1:2:0.5); IR (KBr): $\nu_{\max}/\text{cm}^{-1}$: 3432 (NH), 3066 (CH aromatic), 2925 (CH aliphatic), 1689 (C=O), 1595 (C=N), 1498 (C=C); ¹H NMR (DMSO- d_6 , 500 MHz): δ_H 1.96 (s, 3H, CH₃), 2.34 (s, 3H, CH₃), 2.61 (s, 3H, CH₃), 6.29 (s, 1H, aromatic protons), 6.63 (d, $J = 8.5$ Hz, 1H, aromatic protons), 6.99 (d, $J = 8.0$ Hz, 1H, aromatic protons), 7.30–7.33 (m, 2H, aromatic protons), 7.42–7.45 (m, 2H, aromatic protons), 7.55–7.61 (m, 2H, aromatic protons), 7.78 (d, $J = 9.5$ Hz, 1H, aromatic protons), 8.10–8.15 (m, 1H, aromatic protons); ¹³C NMR (DMSO- d_6 , 125 MHz): δ_C 13.58, 16.72, 22.09, 102.38, 104.61, 106.69, 110.90, 115.13, 122.53, 123.57, 129.95, 132.15, 129.95, 132.15, 137.28, 148.07, 154.63, 168.85; MS (EI, 70 eV): m/z (%) 439.2 (100) [M+1]⁺, 440.2 (25) [M+2]⁺. Anal. calcd. for C₂₆H₂₂N₄O₃ (FW: 438): C, 71.22; H, 5.06; N, 12.78. Found: C, 71.39; H, 5.21; N, 12.66.

4.2.2 | General procedure for the synthesis of compounds 27–32

A solution of compounds **21** (0.40 g, 1 mmol), **22** (0.40 g, 1 mmol), **23** (0.41 g, 1 mmol), **24** (0.38 g, 1 mmol), **25** (0.41 g, 1 mmol), or **26** (0.43 g, 1 mmol) dissolved in dry ethanol (30 ml) and concentrated sulfuric acid (0.98 g, 10 mmol) was allowed to reflux for 5–8 h. Completion of the reaction was monitored using TLC. After cooling to room temperature, the reaction mixture was poured on ice/water and neutralized using diluted ammonium hydroxide. The precipitated crude product was collected by filtration, dried, and purified by recrystallization from methanol to give compounds **27–32**, respectively.

Ethyl-2-(3-methyl-5-morpholino-1-phenyl-1H-pyrazol-4-yl)-1H-benzo[d]imidazole-5-carboxylate (27)

Yield = 37.7%; mp: 118–121°C; $R_f = 0.66$ (petroleum ether/EtOAc = 1:4); IR (KBr): $\nu_{\max}/\text{cm}^{-1}$: 3433 (NH), 3064 (CH aromatic), 2923 (CH aliphatic), 1714 (C=O), 1628 (C=N), 1592 (C=C); ¹H NMR (DMSO- d_6 , 500 MHz): δ_H 1.36 (t, $J = 7.0$ Hz, 3H, CH₃), 2.30 (s, 3H, CH₃), 2.94 (brs, 4H, H3, H5 morpholine protons), 3.51 (brs, 4H, H2, H6 morpholine protons), 4.34 (q, $J = 7.0$ Hz, 2H, CH₂), 7.44–7.55 (m, 1H, aromatic proton), 7.57–7.59 (m, 2H, aromatic protons), 7.66 (d, $J = 8.0$ Hz, 2H, aromatic proton), 7.96 (d, $J = 8.5$ Hz, 1H, aromatic proton), 8.12 (d, $J = 8.5$ Hz, 1H, aromatic proton), 8.40 (s, 1H, aromatic proton); ¹³C NMR (DMSO- d_6 , 125 MHz): δ_C 13.62, 14.94, 50.61, 61.77, 66.67, 103.38, 123.00, 124.40, 125.14, 126.02, 128.73, 129.60, 130.06, 130.32, 139.52, 148.74, 149.90, 150.22, 167.59; MS (EI, 70 eV): m/z (%) 432.2 (100) [M+1]⁺, 433.2 (27) [M+2]⁺. Anal. calcd. for C₂₄H₂₅N₅O₃ (FW: 431): C, 66.81; H, 5.84; N, 16.23. Found: C, 66.65; H, 5.75; N, 16.19.

Ethyl-2-[3-methyl-1-phenyl-5-(piperidin-1-yl)-1H-pyrazol-4-yl]-1H-benzo[d]imidazole-5-carboxylate (28)

Yield = 56.6%; mp: 270–272°C; $R_f = 0.80$ (petroleum ether/EtOAc/ethanol = 1:3:0.5); IR (KBr): $\nu_{\max}/\text{cm}^{-1}$: 3433 (NH), 3058 (CH aromatic), 2939 (CH aliphatic), 1720 (C=O), 1628 (C=N), 1592 (C=C); ^1H NMR (DMSO- d_6 , 500 MHz): δ_{H} 1.37 (t, $J = 7.0$ Hz, 3H, CH₃), 1.38–1.40 (m, 6H, H3, H4, H5 piperidine protons), 2.31 (s, 3H, CH₃), 2.88–2.90 (m, 4H, H2, H6 piperidine protons), 4.38 (q, $J = 7.0$ Hz, 2H, CH₂), 7.44–7.47 (m, 1H, aromatic proton), 7.55–7.59 (m, 2H, aromatic protons), 7.66 (d, $J = 8.0$ Hz, 1H, aromatic protons), 7.96 (d, $J = 8.5$ Hz, 1H, aromatic protons), 8.12 (d, $J = 8.5$ Hz, 1H, aromatic protons), 8.40 (s, 1H, aromatic proton); ^{13}C NMR (DMSO- d_6 , 125 MHz): δ_{C} 13.64, 15.09, 23.31, 25.79, 51.09, 62.12, 94.53, 114.61, 116.06, 124.86, 126.55, 128.82, 129.64, 132.81, 136.20, 140.11, 146.97, 148.97, 152.67, 165.44; MS (EI, 70 eV): m/z (%) 430.2 (100) [M+1]⁺, 431.2 [M+2]⁺. Anal. calcd. for C₂₅H₂₇N₅O₂ (FW: 429): C, 69.91; H, 6.34; N, 16.31. Found C, 69.81; H, 6.27; N, 16.28.

Ethyl-2-[3-methyl-5-(4-methylpiperazin-1-yl)-1-phenyl-1H-pyrazol-4-yl]-1H-benzo[d]imidazole-5-carboxylate (29)

Yield = 40%; mp: 106–108°C; $R_f = 0.62$ (petroleum ether/EtOAc/ethanol = 1:3:0.5); ^1H NMR (DMSO- d_6 , 400 MHz): 1.36 (t, $J = 7.1$ Hz, 3H, CH₃), 2.16 (s, 3H, CH₃), 2.28–2.30 (m, 7H, CH₃ + 4H piperazine protons), 2.95 (brs, 4H, piperazine protons), 4.34 (q, $J = 7.1$ Hz, 2H, CH₂), 7.39–7.43 (m, 1H, aromatic proton), 7.52–7.56 (m, 2H, aromatic protons), 7.69–7.76 (m, 3H, aromatic protons), 7.83–7.89 (m, 1H, aromatic proton), 8.27 (s, 1H, aromatic proton), 12.67 (brs, 1H, NH); ^{13}C NMR (DMSO- d_6 , 100 MHz): δ_{C} 13.67, 14.72, 40.56, 49.79, 54.64, 60.94, 104.10, 124.60, 127.86, 129.43, 139.59, 147.92, 149.66, 166.77. Anal. calcd. for C₂₅H₂₈N₆O₂ (FW: 444): C, 67.55; H, 6.35; N, 18.91. Found: C, 67.48; H, 6.26; N, 18.89.

Ethyl-2-[3-methyl-1-phenyl-5-(pyrrolidin-1-yl)-1H-pyrazol-4-yl]-1H-benzo[d]imidazole-5-carboxylate (30)

Yield = 47.1%; mp: 268–270°C; $R_f = 0.68$ (petroleum ether/EtOAc = 0.5:4); IR (KBr): $\nu_{\max}/\text{cm}^{-1}$: 3425 (NH), 3058 (CH aromatic), 2976 (CH aliphatic), 1718 (C=O), 1627 (C=N), 1591 (C=C); ^1H NMR (DMSO- d_6 , 500 MHz): δ_{H} 1.34 (t, $J = 7.5$ Hz, 3H, CH₃), 1.70–1.74 (m, 4H, pyrrolidine protons), 2.25 (s, 3H, CH₃), 2.97–2.99 (m, 2H, pyrrolidine protons), 4.32 (q, $J = 8.0$ Hz, 2H, CH₂), 7.37–7.40 (m, 1H, aromatic proton), 7.49–7.52 (m, 2H, aromatic protons), 7.57 (d, $J = 7.5$ Hz, 2H, aromatic protons), 7.65 (d, $J = 8.5$ Hz, 1H, aromatic proton), 7.80 (d, $J = 8.5$ Hz, 1H, aromatic proton), 8.17 (s, 1H, aromatic proton); ^{13}C NMR (DMSO- d_6 , 125 MHz): δ_{C} 13.64, 15.08, 25.62, 51.10, 60.47, 122.84, 124.58, 127.37, 129.95, 140.13, 148.37, 167.10; MS (EI, 70 eV): m/z (%) 416.2 (100) [M+1]⁺. Anal. calcd. for C₂₄H₂₅N₅O₂ (FW: 415): C, 69.38; H, 6.06; N, 16.86. Found: C, 69.28; H, 6.16; N, 16.95.

Ethyl-2-(3-methyl-5-phenoxy-1-phenyl-1H-pyrazol-4-yl)-1H-benzo[d]imidazole-5-carboxylate (31)

Yield = 45%; mp: 97–99°C; $R_f = 0.61$ (petroleum ether/EtOAc = 1:3); IR (KBr): $\nu_{\max}/\text{cm}^{-1}$: 3433 (NH), 3064 (CH aromatic), 2923

(CH aliphatic), 1714 (C=O), 1628 (C=N), 1592 (C=C); ^1H NMR (DMSO- d_6 , 500 MHz): δ_{H} 1.35 (t, $J = 7.0$ Hz, 3H, CH₃), 2.63 (s, 3H, CH₃), 4.32 (q, $J = 7.5$ Hz, 2H, CH₂), 6.93–6.98 (m, 2H, aromatic protons), 7.18–7.22 (m, 2H, aromatic protons), 7.35–7.38 (m, 2H, aromatic protons), 7.46–7.49 (m, 2H, aromatic protons), 7.64–7.69 (m, 3H, aromatic protons), 7.87 (d, $J = 8.5$ Hz, 1H, aromatic proton), 8.17 (s, 1H, aromatic proton); ^{13}C NMR (DMSO- d_6 , 125 MHz): δ_{C} 14.26, 16.01, 61.71, 115.85, 123.24, 125.25, 128.91, 130.33, 130.65, 137.45, 148.79, 155.86, 166.07; MS (EI, 70 eV): m/z (%) 439.1 (100) [M+1]⁺, 440.2 (25) [M+2]⁺. Anal. calcd. for C₂₆H₂₂N₄O₃ (FW: 438): C, 71.22; H, 5.06; N, 12.78. Found: C, 71.31; H, 5.00; N, 12.69.

Ethyl-2-[5-(2,5-dimethylphenoxy)-3-methyl-1-phenyl-1H-pyrazol-4-yl]-1H-benzo[d]imidazole-5-carboxylate (32)

Yield = 40%; mp: 101–103°C; $R_f = 0.57$ (petroleum ether/EtOAc = 1:4.5); ^1H NMR (DMSO- d_6 , 500 MHz): δ_{H} 1.34 (t, $J = 9.0$ Hz, 3H, CH₃), 1.97 (s, 3H, CH₃), 2.28 (s, 3H, CH₃), 2.58 (s, 3H, CH₃), 4.34 (q, $J = 9.0$ Hz, 2H, CH₂), 6.43–6.46 (m, 1H, aromatic proton), 6.59–6.62 (m, 1H, aromatic proton), 6.94–6.97 (m, 1H, aromatic proton), 7.37–7.40 (m, 1H, aromatic proton), 7.47–7.50 (m, 2H, aromatic protons), 7.59–7.61 (m, 2H, aromatic protons), 7.73–7.76 (m, 1H, aromatic proton), 7.94–7.97 (m, 1H, aromatic proton), 8.22 (s, 1H, aromatic proton); ^{13}C NMR (DMSO- d_6 , 125 MHz): δ_{C} 14.34, 14.61, 18.91, 20.74, 61.50, 96.61, 114.94, 115.06, 115.33, 116.16, 121.54, 123.31, 123.99, 125.30, 126.10, 128.68, 129.63, 129.84, 131.69, 137.11, 137.14, 145.68, 148.69, 148.93, 149.21, 153.65, 166.01, 167.40. Anal. calcd. for C₂₈H₂₆N₄O₃ (FW: 466): C, 72.09; H, 5.62; N, 12.01. Found: C, 72.15; H, 5.73; N, 12.09.

4.2.3 | General procedure for the synthesis of compounds 33–36

A solution of compounds **27** (1.70 g, 5 mmol), **28** (2.14 g, 5 mmol), **30** (2.07 g, 5 mmol), or **31** (2.19 g, 5 mmol) and hydrazine hydrate (1.00 g, 20 mmol) in ethanol (30 ml) was refluxed for 7–9 h. After cooling to room temperature, the reaction mixture was concentrated to one-third by evaporation of the solvent under reduced pressure. The remaining precipitate was washed with cold water and collected by filtration and left to dry. The crude product was further purified by recrystallization from ethanol to give compounds **33**, **34**, **35**, or **36**, respectively.

2-(3-Methyl-5-morpholino-1-phenyl-1H-pyrazol-4-yl)-1H-benzo[d]imidazole-5-carbohydrazide (33)

Yield = 77%; mp: 170–173°C; $R_f = 0.12$ (petroleum ether/EtOAc/ethanol = 1:2:0.5); IR (KBr): $\nu_{\max}/\text{cm}^{-1}$: 3407 (NH), 3097 (CH aromatic), 2968 (CH aliphatic), 1623 (C=N), 1530 (C=C); ^1H NMR (DMSO- d_6 , 500 MHz): δ_{H} 2.27 (s, 3H, CH₃), 2.91–2.92 (m, 4H, H3, H5 morpholine protons), 3.48–3.50 (m, 4H, H2, H6 morpholine protons), 4.80 (brs, 2H, NH₂, D₂O exchangeable), 7.38–7.41 (m, 1H, aromatic

protons), 7.51–7.54 (m, 3H, aromatic protons), 7.72 (d, $J = 7.5$ Hz, 3H, aromatic protons), 8.05–8.17 (m, 1H, aromatic protons), 9.75 (s, 1H, NH, D₂O exchangeable), 12.56 (brs, 1H, NH, D₂O exchangeable); ¹³C NMR (DMSO-*d*₆, 125 MHz): δ_C 13.32, 50.25, 66.14, 103.27, 125.11, 127.97, 129.42, 138.78, 147.83, 150.11, 168.02; MS (EI, eV): m/z (%) 418.1 (100) [M+1]⁺, 419.2 (25) [M+2]⁺. Anal. calcd. for C₂₂H₂₃N₇O₂ (FW: 417): C, 63.30; H, 5.55; N, 23.49. Found: C, 63.19; H, 5.28; N, 23.32.

2-[3-Methyl-1-phenyl-5-(piperidin-1-yl)-1H-pyrazol-4-yl]-1H-benzo[d]imidazole-5-carbohydrazide (34)

Yield = 45%; mp: 164–166°C; $R_f = 0.43$ (petroleum ether/EtOAc/ethanol = 1:2:0.5); 3458, 3418, 3392 (NH, NH₂), 3097 (CH aromatic), 2928 (CH aliphatic), 1623 (C=N), 1592 (C=C); ¹H NMR (DMSO-*d*₆, 500 MHz): δ_H 1.37 (brs, 6H, H3, H4, H5 piperidine protons), 2.22 (s, 3H, CH₃), 2.83–2.84 (m, 4H, H2, H6 piperidine protons), 4.67 (brs, 2H, NH₂, D₂O exchangeable), 7.36–7.39 (m, 1H, aromatic proton), 7.50–7.53 (m, 2H, aromatic protons), 7.61–7.62 (m, 1H, aromatic protons), 7.70–7.73 (m, 3H, aromatic protons), 8.11 (brs, 1H, aromatic protons), 9.74 (s, 1H, NH, D₂O exchangeable), 12.52 (brs, 1H, NH, D₂O exchangeable); ¹³C NMR (DMSO-*d*₆, 125 MHz): δ_C 13.19, 23.33, 25.18, 50.98, 103.17, 123.82, 127.13, 128.95, 139.48, 147.47, 150.03, 166.67; MS (EI, eV): m/z (%) 416 (100) [M+1]⁺. Anal. calcd. for C₂₃H₂₅N₇O (FW: 415): C, 66.49; H, 6.06; N, 23.60. Found: C, 66.59; H, 6.16; N, 23.75.

2-[3-Methyl-1-phenyl-5-(pyrrolidin-1-yl)-1H-pyrazol-4-yl]-1H-benzo[d]imidazole-5-carbohydrazide (35)

Yield = 45%; mp: 248–250°C; $R_f = 0.48$ (petroleum ether/EtOAc/ethanol = 1:2:0.25); IR (KBr): $\nu_{\max}/\text{cm}^{-1}$: 3455, 3408, 3397 (NH, NH₂), 2932 (CH aliphatic), 1630 (C=O), 1514 (C=N), 1450 (C=C); ¹H NMR (DMSO-*d*₆, 500 MHz): δ_H 1.69–1.72 (m, 4H, H3, H4 pyrrolidine protons), 2.22 (s, 3H, CH₃), 2.94–2.97 (m, 4H, H2, H5 pyrrolidine protons), 4.64 (brs, 2H, NH₂), 7.37–7.40 (m, 1H, aromatic proton), 7.49–7.53 (m, 3H, aromatic protons), 7.67 (d, $J = 7.5$ Hz, 2H, aromatic protons), 7.63–7.74 (m, 1H, aromatic protons), 8.00–8.14 (m, 1H, aromatic protons), 9.74 (brs, 1H, NH), 12.44 (brs, 1H, NH); ¹³C NMR (DMSO-*d*₆, 125 MHz): δ_C 13.69, 25.54, 50.88, 101.10, 111.00, 111.19, 117.88, 118.34, 124.75, 127.72, 129.53, 140.38, 148.26, 168.00; MS (EI, eV): m/z (%) 402.2 (70) [M+1]⁺, 403.2 (30) [M+2]⁺. Anal. calcd. for C₂₂H₂₃N₇O (FW: 401): C, 65.82; H, 5.77; N, 24.42. Found: C, 65.62; H, 5.61; N, 24.29.

2-(3-Methyl-5-phenoxy-1-phenyl-1H-pyrazol-4-yl)-1H-benzo[d]imidazole-5-carbohydrazide (36)

Yield = 46%; mp: 92–94°C; $R_f = 0.62$ (petroleum ether/EtOAc/ethanol = 1:4:0.5); ¹H NMR (DMSO-*d*₆, 400 MHz): δ_H 2.62 (s, 3H, CH₃), 6.92–6.99 (m, 3H, aromatic protons), 7.16–7.24 (m, 2H, aromatic protons), 7.33–7.35 (m, 2H, aromatic protons), 7.44–7.48 (m, 2H, aromatic protons), 7.55–7.57 (m, 2H, aromatic protons), 7.62–7.68 (m, 2H, aromatic protons). Anal. calcd. for C₂₄H₂₀N₆O₂ (FW: 424): C, 67.91; H, 4.75; N, 19.80. Found: C, 67.85; H, 4.86; N, 19.69.

4.2.4 | General procedure for the synthesis of compounds 37–41

A solution of 4-hydroxybenzaldehyde (0.14 g, 1.19 mmol), 3-hydroxybenzaldehyde (0.14 g, 1.19 mmol), vanillin (0.18 g, 1.19 mmol), 4-chlorobenzaldehyde (0.16, 1.19 mmol), or furfural (0.11 g, 1.19 mmol) in absolute ethanol (20 ml) was added to a solution of compound 33 (0.5 g, 1.19 mmol) in absolute ethanol (10 ml) and glacial acetic acid (2 ml). The mixture was refluxed for 6–8 h. Completion of the reaction was monitored by TLC. After cooling to room temperature, the mixture was poured on crushed ice, neutralized by diluted ammonia, and the crude product was filtered off and dried. The product was recrystallized from ethanol to give compounds 37–41, respectively.

N'-(4-Hydroxybenzylidene)-2-(3-methyl-5-morpholino-1-phenyl-1H-pyrazol-4-yl)-1H-benzo[d]imidazole-5-carbohydrazide (37)

Yield = 32%; mp: 196–198°C; $R_f = 0.43$ (petroleum ether/EtOAc/ethanol = 1:3:0.25); IR (KBr): $\nu_{\max}/\text{cm}^{-1}$: 3426 (NH), 3050 (CH aromatic), 2963 (CH aliphatic), 1741 (C=O), 1640 (C=N), 1593 (C=C); ¹H NMR (DMSO-*d*₆, 500 MHz): δ_H 2.30 (s, 3H, CH₃), 2.95 (s, 4H, H3, H5 morpholine protons), 3.51 (s, 4H, H2, H6 morpholine protons), 6.85–6.86 (m, 2H, aromatic protons), 7.42–7.43 (m, 2H, aromatic proton), 7.53–7.66 (m, 4H, aromatic proton), 7.73–7.84 (m, 3H, aromatic protons), 8.14 (s, 1H, aromatic proton), 8.36–8.40 (m, 1H, aromatic proton), 9.93 (s, 1H, NH), 11.70 (s, 1H, NH), 12.62 (s, 1H, OH); ¹³C NMR (DMSO-*d*₆, 125 MHz): δ_C 14.18, 50.47, 66.42, 104.40, 118.62, 121.48, 123.44, 124.91, 125.71, 129.63, 134.24, 137.85, 140.11, 143.60, 146.70, 147.85, 149.81, 160.01, 163.71; MS (EI, eV): m/z (%) 522.2 (100) [M+1]⁺. Anal. calcd. for C₂₉H₂₇N₇O₃ (FW: 521): C, 66.78; H, 5.22; N, 18.80. Found: C, 66.69; H, 5.38; N, 18.92.

N'-(3-Hydroxybenzylidene)-2-(3-methyl-5-morpholino-1-phenyl-1H-pyrazol-4-yl)-1H-benzo[d]imidazole-5-carbohydrazide (38)

Yield = 41%; mp: 218–220°C; $R_f = 0.58$ (petroleum ether/EtOAc/methanol = 1:3:0.5); IR (KBr): $\nu_{\max}/\text{cm}^{-1}$: 3366 (NH), 3068 (CH aromatic), 2964 (CH aliphatic), 1653 (C=O), 1590 (C=N), 1541 (C=C); ¹H NMR (DMSO-*d*₆, 500 MHz): δ_H 2.29 (s, 3H, CH₃), 2.94 (s, 4H, H3, H5 morpholine protons), 3.51 (s, 4H, H2, H6 morpholine protons), 6.84 (s, 1H, aromatic protons), 7.11 (s, 1H, aromatic protons), 7.23 (s, 2H, aromatic protons), 7.41 (s, 1H, aromatic proton), 7.54 (s, 2H, aromatic proton), 7.66–7.88 (m, 4H, aromatic protons), 8.15–8.41 (m, 2H, 1H aromatic proton + CH=N), 9.65 (s, 1H, OH), 11.86 (brs, 1H, NH), 12.64 (brs, 1H, NH). Anal. calcd. for C₂₉H₂₇N₇O₃ (FW: 521): C, 66.78; H, 5.22; N, 18.80. Found: C, 66.68; H, 5.10; N, 18.65.

N'-(4-Hydroxy-3-methoxybenzylidene)-2-(3-methyl-5-morpholino-1-phenyl-1H-pyrazol-4-yl)-1H-benzo[d]imidazole-5-carbohydrazide (39)

Yield = 35%; mp: 191–193°C; $R_f = 0.33$ (petroleum ether/EtOAc/ethanol = 1:3:0.5); IR (KBr): $\nu_{\max}/\text{cm}^{-1}$: 3426 (NH), 3090 (CH

aromatic), 2966 (CH aliphatic), 1633 (C=O), 1593 (C=N), 1509 (C=C); ^1H NMR (DMSO- d_6 , 500 MHz): δ_{H} 2.29 (s, 3H, CH₃), 2.94 (brs, 4H, H3, H5 morpholine protons), 3.51 (brs, 4H, H2, H6 morpholine protons), 3.84 (s, 3H, OCH₃), 6.85 (d, J = 8.0 Hz, 1H, aromatic proton), 7.08 (d, J = 8.0 Hz, 1H, aromatic proton), 7.39–7.42 (m, 1H, aromatic protons), 7.52–7.55 (m, 2H, aromatic proton), 7.64–7.82 (m, 4H, aromatic proton), 8.34–8.38 (m, 2H, aromatic proton), 11.72 (s, 1H, NH); ^{13}C NMR (DMSO- d_6 , 125 MHz): δ_{C} 13.27, 49.97, 55.54, 65.98, 108.84, 115.44, 122.05, 124.16, 124.16, 125.94, 127.43, 129.01, 139.07, 147.49, 148.06, 148.88, 163.27; MS (EI, eV): m/z (%) 552.2 (100) [M+1]⁺, 553.2 (30) [M+2]⁺. Anal. calcd. for C₃₀H₂₉N₇O₄ (FW: 551): C, 65.32; H, 5.30; N, 17.78. Found: C, 65.43; H, 5.45; N, 17.86.

N'-(4-Chlorobenzylidene)-2-(3-methyl-5-morpholino-1-phenyl-1H-pyrazol-4-yl)-1H-benzo[d]imidazole-5-carbohydrazide (40)

Yield = 45%; mp: 142–144°C; R_f = 0.58 (petroleum ether/EtOAc/methanol = 1:3:0.5); IR (KBr): $\nu_{\text{max}}/\text{cm}^{-1}$: 3387 (NH), 3069 (CH aromatic), 2920 (CH aliphatic), 1657 (C=O), 1626, 1594 (C=N), 1540 (C=C); ^1H NMR (DMSO- d_6 , 400 MHz): δ_{H} 2.31 (s, 3H, CH₃), 2.94 (brs, 4H, H3, H5 morpholine protons), 3.53 (brs, 4H, H2, H6 morpholine protons), 7.37–7.54 (m, 6H, aromatic protons), 7.75–8.17 (m, 5H, aromatic protons), 8.51–8.71 (m, 2H, 1H aromatic proton + CH=N), 11.99 (brs, 1H, NH), 12.62 (brs, 1H, NH). Anal. calcd. for C₂₉H₂₆ClN₇O₂ (FW: 540): C, 64.50; H, 4.85; Cl, 6.57; N, 18.16. Found: C, 64.68; H, 4.99; Cl, 6.62; N, 18.25.

N'-[(Furan-3-yl)methylene]-2-(3-methyl-5-morpholino-1-phenyl-1H-pyrazol-4-yl)-1H-benzo[d]imidazole-5-carbohydrazide (41)

Yield = 36%; mp: 151–153°C; R_f = 0.46 (petroleum ether/EtOAc/ethanol = 1:2:0.25); IR (KBr): $\nu_{\text{max}}/\text{cm}^{-1}$: 3430 (NH), 3097 (CH aromatic), 2963 (CH aliphatic), 1628 (C=N), 1593 (C=N), 1531 (C=C); ^1H NMR (DMSO- d_6 , 500 MHz): δ_{H} 2.29 (s, 3H, CH₃), 2.94 (brs, 4H, H3, H5 morpholine protons), 3.50–3.51 (m, 4H, H2, H6 morpholine protons), 6.85 (d, J = 8.0 Hz, 1H, aromatic proton), 7.08 (d, J = 8.0 Hz, 1H, aromatic proton), 7.33 (s, 1H, aromatic proton), 7.39–7.43 (m, 1H, aromatic proton), 7.52–7.56 (m, 1H, aromatic protons), 7.64–7.82 (m, 4H, aromatic proton), 8.13–8.38 (m, 2H, 1H aromatic proton + CH=N), 11.72 (s, 1H, NH), 12.59 (brs, 1H, NH). Anal. calcd. for C₂₇H₂₅N₇O₃ (FW: 495): C, 65.44; H, 5.09; N, 19.79. Found: C, 65.60; H, 5.18; N, 19.85.

4.2.5 | General procedure for the synthesis of compounds 42–45

A solution of 4-hydroxybenzaldehyde (0.15 g, 1.24 mmol), 3-hydroxybenzaldehyde (0.15 g, 1.24 mmol), vanillin (0.19 g, 1.24 mmol), or 4-chlorobenzaldehyde (0.17 g, 1.24 mmol) in absolute ethanol (20 ml) was added to a solution of compound 35 (0.5 g, 1.24 mmol) in absolute ethanol (10 ml) and glacial acetic acid (2 ml). The mixture was refluxed for 6–8 h. Completion of the reaction was monitored by TLC. After cooling to room temperature, the mixture

was poured on crushed ice, neutralized by diluted ammonia, and the crude product was filtered off and dried. The product was recrystallized from ethanol to give compounds 42–45, respectively.

N'-(4-Hydroxybenzylidene)-2-[3-methyl-1-phenyl-5-(pyrrolidin-1-yl)-1H-pyrazol-4-yl]-1H-benzo[d]imidazole-5-carbohydrazide (42)

Yield = 47%; mp: 196–198°C; R_f = 0.43 (petroleum ether/EtOAc/ethanol = 1:2:0.25); IR (KBr): $\nu_{\text{max}}/\text{cm}^{-1}$: 3433 (NH), 2961 (CH aliphatic), 1630 (C=O), 1531 (C=N), 1501 (C=C); ^1H NMR (DMSO- d_6 , 500 MHz): δ_{H} 1.71 (s, 4H, H3, H4 pyrrolidine protons), 2.24 (s, 3H, CH₃), 2.97 (s, 4H, H2, H5 pyrrolidine protons), 6.85 (d, J = 8.0 Hz, 2H, aromatic protons), 7.37–7.40 (m, 1H, aromatic proton), 7.49–7.52 (m, 2H, aromatic protons), 7.57 (d, J = 7.5 Hz, 4H, aromatic protons), 7.65–7.69 (m, 1H, aromatic proton), 7.81 (d, J = 8.0 Hz, 1H, aromatic proton), 8.22 (s, 1H, aromatic proton), 8.39 (s, 1H, CH=N), 9.94 (s, 1H, NH), 11.70 (s, 1H, OH); ^{13}C NMR (DMSO- d_6 , 125 MHz): δ_{C} 13.30, 25.13, 50.47, 115.73, 124.37, 125.53, 127.32, 128.79, 129.09, 139.92, 147.48, 147.84, 159.33, 163.32; MS (EI, eV): m/z (%) 506.20 (100) [M+1]⁺, 507.3 (27) [M+2]⁺. Anal. calcd. for C₂₉H₂₇N₇O₂ (FW: 505): C, 68.89; H, 5.38; N, 19.39. Found: C, 68.72; H, 5.24; N, 19.22.

N'-(3-Hydroxybenzylidene)-2-[3-methyl-1-phenyl-5-(pyrrolidin-1-yl)-1H-pyrazol-4-yl]-1H-benzo[d]imidazole-5-carbohydrazide (43)

Yield = 40%; mp: 187–189°C; R_f = 0.70 (petroleum ether/EtOAc/ethanol = 0.5:2:0.5); IR (KBr): $\nu_{\text{max}}/\text{cm}^{-1}$: 3428 (NH), 2967 (CH aliphatic), 1628 (C=O), 1586 (C=N), 1541 (C=C); ^1H NMR (DMSO- d_6 , 500 MHz): δ_{H} 1.71 (s, 4H, H3, H4 pyrrolidine protons), 2.24 (s, 3H, CH₃), 2.98 (s, 4H, H2, H5 pyrrolidine protons), 6.83 (d, J = 7.0 Hz, 1H, aromatic proton), 7.10 (d, J = 7.5 Hz, 1H, aromatic protons), 7.22–7.27 (m, 2H, aromatic proton), 7.37–7.40 (m, 1H, aromatic protons), 7.49–7.52 (m, 2H, aromatic protons), 7.57–7.61 (m, 3H, aromatic proton), 7.73–7.81 (m, 2H, aromatic proton + CH=N), 9.65 (brs, 1H, NH), 11.83 (s, 1H, OH), 12.51 (s, 1H, NH); ^{13}C NMR (DMSO- d_6 , 125 MHz): δ_{C} 13.31, 25.13, 50.46, 112.58, 117.30, 118.75, 124.35, 127.31, 129.09, 129.90, 129.96, 135.83, 139.92, 147.82, 157.71, 163.54; MS (EI, eV): m/z (%) 506.2 (100) [M+1]⁺, 507.3 (25) [M+2]⁺. Anal. calcd. for C₂₉H₂₇N₇O₂ (FW: 505): C, 68.89; H, 5.38; N, 19.39. Found: C, 68.95; H, 5.45; N, 19.48.

N'-(4-Hydroxy-3-methoxybenzylidene)-2-[3-methyl-1-phenyl-5-(pyrrolidin-1-yl)-1H-pyrazol-4-yl]-1H-benzo[d]imidazole-5-carbohydrazide (44)

Yield = 45%; mp: 162–164°C; R_f = 0.14 (petroleum ether/EtOAc/ethanol = 1:2:0.5); IR (KBr): $\nu_{\text{max}}/\text{cm}^{-1}$: 3434 (NH), 2925 (CH aliphatic), 1632 (C=O), 1511 (C=N), 1456 (C=C); ^1H NMR (DMSO- d_6 , 500 MHz): δ_{H} 1.70–1.73 (m, 4H, H3, H4 pyrrolidine protons), 2.23 (s, 3H, CH₃), 2.96–2.99 (m, 4H, H2, H5 pyrrolidine protons), 3.84 (s, 3H, OCH₃), 6.85 (d, J = 8.0 Hz, 1H, aromatic protons), 7.08 (d, J = 8.0 Hz, 1H, aromatic proton), 7.33 (s, 1H, aromatic proton), 7.38–7.45 (m, 1H, aromatic protons), 7.56–7.53 (m, 2H, aromatic proton), 7.57 (d, J = 7.5 Hz, 2H, aromatic proton), 7.65 (brs, 1H, aromatic proton), 7.80 (d, J = 8.0 Hz, 1H, aromatic proton), 8.21 (brs, 1H), 8.38 (s, 1H), 9.55 (s, 1H), 11.70 (s, 1H), 12.54 (s, 1H, NH); ^{13}C NMR (DMSO- d_6 ,

125 MHz): δ_C 13.17, 25.41, 50.58, 55.99, 109.48, 115.59, 123.03, 125.08, 1216.23, 127.05, 128.20, 129.68, 140.00, 148.38, 148.56, 148.95, 149.10; MS (EI, eV): m/z (%) 536.2 (100) $[M+1]^+$, 537.3 (25) $[M+2]^+$. Anal. calcd. for $C_{30}H_{29}N_7O_3$ (FW: 535) C, 67.27; H, 5.46; N, 18.31. Found: C, 67.35; H, 5.55; N, 18.21.

N'-(4-Chlorobenzylidene)-2-[3-methyl-1-phenyl-5-(pyrrolidin-1-yl)-1H-pyrazol-4-yl]-1H-benzo[d]imidazole-5-carbohydrazide (45)

Yield = 48%; mp: 136–139°C; R_f = 0.57 (petroleum ether/EtOAc/ethanol = 1:2:1); IR (KBr): ν_{max}/cm^{-1} : 3433 (NH), 2961 (CH aliphatic), 1630 (C=O), 1531 (C=N), 1501 (C=C); 1H NMR (DMSO- d_6 , 500 MHz): δ_H 1.70–1.73 (m, 4H, H3, H4 pyrrolidine protons), 2.24 (s, 3H, CH₃), 2.97–2.99 (m, 4H, H2, H5 pyrrolidine protons), 7.37–7.40 (m, 1H, aromatic proton), 7.49–7.53 (m, 4H, aromatic protons), 7.58 (d, J = 7.5 Hz, 2H, aromatic protons), 7.67 (d, J = 8.0 Hz, 1H, aromatic proton), 7.76 (d, J = 8.0 Hz, 2H, aromatic proton), 7.83 (d, J = 8.0 Hz, 1H, aromatic proton), 8.25 (s, 1H, aromatic proton), 8.49 (s, 1H, CH=N), 11.97 (s, 1H, NH); ^{13}C NMR (DMSO- d_6 , 125 MHz): δ_C 13.64, 25.88, 51.06, 99.25, 122.82, 125.54, 127.30, 128.66, 129.79, 129.93, 130.13, 130.24, 132.11, 133.76, 135.77, 140.44, 147.80, 149.03, 149.29, 149.61, 165.50; MS (EI, eV): m/z (%) 524 (100) $[M]^+$, 526 (25) $[M+2]^+$. Anal. calcd. for $C_{29}H_{26}ClN_7O$ (FW: 524): C, 66.47; H, 5.00; Cl, 6.77; N, 18.71. Found C, 66.30; H, 5.18; Cl, 6.89; N, 18.82.

4.3 | Biological evaluation

4.3.1 | Molecular docking

The structure of SphK1 (PDB ID: 4V24) was retrieved from the Protein Data Bank (PDB). The key amino acids of the active site were identified using data in PDBsum. Molecular docking studies of the newly synthesized compounds with SphK1 were performed to gain insight into the predicted binding affinity and interaction patterns. The 2D and 3D structures of the synthesized compounds were generated using the Chem Draw Ultra v12.0. AutoDock Tools^[70] was used for the preparation of docking files supported by AutoDock Vina^[70]. In this study, we have performed site-specific molecular docking. The docking was done within 15 Å diameters from the reference PF-543 ligand. The binding site of the crystal structure of SphK1 is composed of the following amino acids: Leu167, Ser168, Ala170, Phe173, Ile174, Val177, Asp178, Phe192, Thr196, Leu259, Leu261, Leu268, Ala274, Phe288, Val290, Leu302, Phe303, Met306, His311, and Ala339. The binding site was defined by including all residues constituting the binding pocket of the reference PF-543 ligand. AutoDock Vina was used for running molecular docking. The docked poses of the newly synthesized compounds with SphK1 were ranked on the basis of the predicted binding affinity and interaction patterns. Intermolecular interactions were studied using PyMol molecular.^[71] The 2D plots for protein–ligand interaction were created using the Discovery Studio Visualizer. The top-ranked compounds selected from the analysis are listed in Table 2.

4.3.2 | Expression and purification of SphK1

The secondary cultures of SphK1 were induced by 1 mM IPTG for 4 h, followed by centrifugation at 7000 rpm for 15 min to get the cell pellet, which was later resuspended in the lysis buffer, and inclusion bodies were prepared as described.^[64] Finally, inclusion bodies were solubilized in the solubilization buffer (pH 8.0) comprising 0.5% sarcosine, 50 mM Tris, and 150 mM NaCl. SphK1 was purified using Ni-NTA affinity chromatography, followed by dialysis for 24 h to get the refolded native protein. The purified protein was loaded on SDS-PAGE and the concentration was calculated using a molar absorption coefficient of $48,275 M^{-1} \cdot cm^{-1}$ at 280 nm on the Jasco V-660 UV-visible spectrophotometer.

4.3.3 | Fluorescence binding studies

The Jasco spectrofluorometer at 25°C was used for the binding studies of all the synthesized compounds. The compounds were first dissolved in DMSO to get the 20 mM stock solution and then diluted to a working concentration of 1 mM in 20 mM Tris and 100 mM NaCl buffer (pH 8.0). The quenching studies were performed with a fixed concentration of SphK1 (5 μ M) and the compounds were added gradually in increasing concentration from the 1 mM stocks into the protein solution until the achievement of saturation point. The emission spectra were recorded from 300 to 400 nm with excitation of SphK1 at 280 nm. The blank titrations (buffer with selected compounds) were subtracted to obtain the final spectra and the quenching data was corrected for the inner filter effect according to the formula: $F = F_{obs} \cdot \text{antilog} [(A_{ex} + A_{em})/2]$, where A_{ex} and A_{em} are the absorbance of the selected compound at the excitation and emission wavelength, respectively.^[72] The quenching spectra obtained for selected compounds were plotted and the inverse correlation between the gradual decrease in the fluorescence intensity with increasing concentration of compounds was used for determining the kinetic parameters (K_a and n) from a modified Stern–Volmer equation (Equation 1) as described,^[73] where F_0 denotes fluorescence intensity of SphK1 without the compound and F denotes the fluorescence intensity of SphK1 at a specific concentration of compound at λ_{max} :

$$\log \frac{(F_0 - F)}{F} = \log K_a + n \log [\text{Compound}]. \quad (1)$$

4.3.4 | Enzyme inhibition assay

A standard Malachite Green (BIOMOL® GREEN reagent) microtiter plate assay was performed to evaluate the inhibitory potential of all the synthesized compounds against SphK1. Briefly, compounds were incubated with SphK1 (4 μ M) for 1 h at 25°C and then freshly prepared ATP (200 μ M) and 10 mM $MgCl_2$ were added to the protein–ligand mixture. The reaction was allowed to proceed for 30 min at 25°C. After the required incubation period, the reaction was ended by adding the

double amount of BIOMOL reagent. Finally, a green-colored complex was formed in 10 min and the absorbance readings were recorded on an ELISA reader at 620 nm. The reaction with ligands, and no protein, was also performed to subtract the background reading of inorganic phosphate. A standard phosphate curve was used to determine the loss in activity of SphK1 in terms of the amount of phosphate released on treatment with increasing concentrations of selected compounds. The inhibition in SphK1 activity was plotted for selected compounds in terms of percentage as described.^[65–67]

ACKNOWLEDGMENTS

This study was supported by the research grant offered by the National Research Centre, Cairo, Egypt, through the internal Project No. 12060119. The authors thank the National Cancer Institute (NCI), NIH, Bethesda, MD, USA, for the performance of the antitumor activity screening through the DTP. Ahmad Abu Turab Naqvi is thankful to the Indian Council of Medical Research, New Delhi, for financial assistance (Project: 45/40/2019-BIO/BMS). This study is funded by the Indian Council of Medical Research (Grant No. ISRM/12(22)/2020).

CONFLICTS OF INTERESTS

The authors declare that there are no conflicts of interests.

ORCID

Shadia A. Galal  <http://orcid.org/0000-0002-0320-1655>

Hoda I. El Diwani  <http://orcid.org/0000-0001-7525-9437>

REFERENCES

- N. J. Pyne, A. El Buri, D. R. Adams, S. Pyne, *Adv. Biol. Regul.* **2018**, *68*, 97. <https://doi.org/10.1016/j.jbior.2017.09.006>
- J. W. Antoon, B. S. Beckman, *Cancer. Biol. Ther.* **2011**, *11*, 647. <https://doi.org/10.4161/cbt.11.7.14921>
- D. Plano, S. Amin, A. K. Sharma, *J. Med. Chem.* **2014**, *57*, 5509. <https://doi.org/10.1021/jm4011687>
- S. Pyne, N. J. Pyne, *Handbook of Experimental Pharmacology*, Springer-Verlag, Vienna **2013**, p. 55. <https://doi.org/10.1007/978-3-7091-1511-4>
- S. Schwalm, J. Pfeilschifter, A. Huwiler, *Biochim. Biophys. Acta, Mol. Cell Biol. Lipids* **2013**, *1831*, 239. <https://doi.org/10.1016/j.bbalip.2012.07.022>
- B. Prager, S. F. Spampinato, R. M. Ransohoff, *Trends Mol. Med.* **2015**, *21*, 354. <https://doi.org/10.1016/j.molmed.2015.03.006>
- R. L. Proia, T. Hla, *J. Clin. Invest.* **2015**, *125*, 1379. <https://doi.org/10.1172/JCI76369>
- Y. Zhang, V. Berka, A. Song, K. Sun, W. Wang, W. Zhang, C. Ning, C. Li, Q. Zhang, M. Bogdanov, D. C. Alexander, M. V. Milburn, M. H. Ahmed, H. Lin, M. Idowu, J. Zhang, G. J. Kato, O. Y. Abdulmalik, W. Zhang, W. Dowhan, R. E. Kellems, P. Zhang, J. Jin, M. Safo, A.-L. Tsai, H. S. Juneja, Y. Xia, *J. Clin. Invest.* **2014**, *124*, 2750. <https://doi.org/10.1172/JCI74604>
- S. P. Reid, S. R. Tritsch, K. Kota, C. Y. Chiang, L. Dong, T. Kenny, E. E. Brueggemann, M. D. Ward, L. H. Cazares, S. Bavari, *Emerging Microbes Infect.* **2015**, *4*, 1. <https://doi.org/10.1038/emi.2015.61>
- G. A. Patwardhan, L. J. Beverly, L. J. Siskind, *J. Bioenerg. Biomembr.* **2016**, *48*, 153. <https://doi.org/10.1007/s10863-015-9602-3>
- S. Ponnusamy, M. Meyers-Needham, C. E. Senkal, S. A. Saddoughi, D. Sentelle, S. P. Selvam, A. Salas, B. Ogretmen, *Future Oncol.* **2010**, *6*, 1603. <https://doi.org/10.2217/fon.10.116>
- S. A. Saddoughi, P. Song, B. Ogretmen, *Subcell. Biochem.* **2008**, *49*, 413. https://doi.org/10.1007/978-1-4020-8831-5_16
- M. L. Berwick, B. A. Dudley, K. Maus, C. E. Chalfant, *Adv. Exp. Med. Biol.* **2019**, *1159*, 65. https://doi.org/10.1007/978-3-030-21162-2_5
- G. Musso, M. Cassader, E. Paschetta, R. Gambino, *Gastroenterology* **2018**, *155*, 282. <https://doi.org/10.1053/j.gastro.2018.06.031>
- M. Maceyka, S. G. Payne, S. Milstien, S. Spiegel, *Biochim. Biophys. Acta, Mol. Cell Biol. Lipids* **2002**, *1585*, 193. [https://doi.org/10.1016/S1388-1981\(02\)00341-4](https://doi.org/10.1016/S1388-1981(02)00341-4)
- H. C. Tsai, M. H. Han, *Drugs* **2016**, *76*, 1067. <https://doi.org/10.1007/s40265-016-0603-2>
- J. Guillermet-Guibert, L. Davenne, D. Pchejetski, N. Saint-Laurent, L. Brizuela, C. Guilbeau-Frugier, M. B. Delisle, O. Cuvillier, C. Susini, C. Bousquet, *Mol. Cancer Ther.* **2009**, *8*, 809. <https://doi.org/10.1158/1535-7163.MCT-08-1096>
- D. Hatoum, N. Haddadi, Y. Lin, N. T. Nassif, E. M. McGowan, *Oncotarget* **2017**, *8*, 36898. <https://doi.org/10.18632/oncotarget.16370>
- A. J. Melendez, E. Carlos-Dias, M. Gosink, J. M. Allen, L. Takacs, *Gene* **2000**, *251*, 19. [https://doi.org/10.1016/S0378-1119\(00\)00205-5](https://doi.org/10.1016/S0378-1119(00)00205-5)
- C. R. Gault, L. M. Obeid, Y. A. Hannun, *Adv. Exp. Med. Biol.* **2010**, *688*, 1. https://doi.org/10.1007/978-1-4419-6741-1_1
- D. Shida, K. Takabe, D. Kapitonov, S. Milstien, S. Spiegel, *Drug Targets* **2008**, *9*, 662. <https://doi.org/10.2174/138945008785132402>
- E. H. Arash, A. Shiban, S. Song, L. Attisano, *EMBO Rep.* **2017**, *18*, 420. <https://doi.org/10.15252/embr.201642455>
- T. Aoyagi, M. Nagahashi, A. Yamada, K. Takabe, *Lymphatic Res. Biol.* **2012**, *10*, 97. <https://doi.org/10.1089/lrb.2012.0010>
- M. G. Bayerl, R. D. Bruggeman, E. J. Conroy, J. A. Hengst, T. S. King, M. Jimenez, D. F. Claxton, J. K. Yun, *Leuk. Lymphoma* **2008**, *49*, 948. <https://doi.org/10.1080/10428190801911654>
- M. Nagahashi, A. Yamada, E. Katsuta, T. Aoyagi, W. C. Huang, K. P. Terracina, N. C. Hait, J. C. Allegood, J. Tsuchida, K. Yuza, M. Nakajima, M. Abe, K. Sakimura, S. Milstien, T. Wakai, S. Spiegel, K. Takabe, *Cancer Res.* **2018**, *78*, 781713. <https://doi.org/10.1158/0008-5472.CAN-17-1423>
- F. Wang, Z. Wu, *Exp. Ther. Med.* **2018**, *15*, 5371. <https://doi.org/10.3892/etm.2018.6086>
- H. Aoki, M. Aoki, E. Katsuta, R. Ramanathan, M. O. Idowu, S. Spiegel, K. Takabe, *J. Surg. Res.* **2016**, *205*, 510. <https://doi.org/10.1016/j.jss.2016.05.034>
- H. Furuya, Y. Shimizu, P. M. Tamashiro, K. Iino, J. Bielawski, O. T. Chan, I. Pagano, T. Kawamori, *J. Transl. Med.* **2017**, *15*, 1. <https://doi.org/10.1186/s12967-017-1220-x>
- S. W. Paugh, B. S. Paugh, M. Rahmani, D. Kapitonov, J. A. Almenara, T. Kordula, S. Milstien, J. K. Adams, R. E. Zipkin, S. Grant, S. Spiegel, *Blood* **2008**, *112*, 1382. <https://doi.org/10.1182/blood-2008-02-138958>
- B. Ogretmen, Y. A. Hannun, *Nat. Rev. Cancer* **2004**, *4*, 604. <https://doi.org/10.1038/nrc1411>
- J. J. Clemens, M. D. Davis, K. R. Lynch, T. L. Macdonald, *Bioorg. Med. Chem. Lett.* **2003**, *13*, 3401. [https://doi.org/10.1016/S0960-894X\(03\)00812-6](https://doi.org/10.1016/S0960-894X(03)00812-6)
- Y. Igarashi, S. Hakomori, T. Toyokuni, B. Dean, S. Fujita, M. Sugimoto, T. Ogawa, K. El-Ghendy, E. Racker, *Biochem* **1989**, *28*, 6796. <https://doi.org/10.1021/bi00443a002>
- J. A. Cohen, F. Barkhof, G. Comi, H. P. Hartung, B. O. Khatiri, X. Montalban, J. Pelletier, R. Capra, P. Gallo, G. Izquierdo, K. Tiel-Wilck, A. de Vera, J. Jin, T. Stites, S. Wu, S. Aradhya, L. Kappos, *N. Engl. J. Med.* **2010**, *362*, 402. <https://doi.org/10.1056/nejmoa0907839>
- L. Kappos, E. W. Radue, P. O'Connor, C. Polman, R. Hohlfeld, P. Calabresi, K. Selmaj, C. Agoropoulou, M. Leyk, L. Zhang-Auberson, P. Burtin, *N. Engl. J. Med.* **2010**, *362*, 387. <https://doi.org/10.1056/NEJMoa0909494>
- M. E. Schnute, M. D. McReynolds, T. Kasten, M. Yates, G. Jerome, J. W. Rains, T. Hall, J. Chrencik, M. Kraus, C. N. Cronin, M. Saabye,

- M. K. Highkin, R. Broadus, S. Ogawa, K. Cukyne, L. E. Zawadzke, V. Peterkin, K. Iyanar, J. A. Scholten, J. Wendling, H. Fujiwara, O. Nemirovskiy, A. J. Wittwer, M. M. Nagiec, *Biochem. J.* **2012**, *444*, 79. <https://doi.org/10.1042/BJ20111929>
- [36] M. E. Schnute, M. D. McReynolds, J. Carroll, J. Chrencik, M. K. Highkin, K. Iyanar, G. Jerome, J. W. Rains, M. Saabye, J. A. Scholten, M. Yates, M. M. Nagiec, *J. Med. Chem.* **2017**, *60*, 2562. <https://doi.org/10.1021/acs.jmedchem.7b00070>
- [37] K. J. French, R. S. Schrecengost, B. D. Lee, Y. Zhuang, S. N. Smith, J. L. Eberly, J. K. Yun, C. D. Smith, *Cancer Res.* **2003**, *63*, 5962.
- [38] P. Gao, Y. K. Peterson, R. A. Smith, C. D. Smith, *PLOS One* **2012**, *7*, e44543. <https://doi.org/10.1371/journal.pone.0044543>
- [39] K. A. O. Gandy, L. M. Obeid, *Biochim. Biophys. Acta, Mol. Cell Biol. Lipids* **1831**, 2013, 157. <https://doi.org/10.1016/j.bbali.2012.07.002>
- [40] J. Wang, S. Knapp, N. J. Pyne, S. Pyne, J. M. Elkins, *ACS Med. Chem. Lett.* **2014**, *5*, 1329. <https://doi.org/10.1016/j.str.2013.02.025>
- [41] Z. Wang, X. Min, S. H. Xiao, S. Johnstone, W. Romanow, D. Meininger, H. Xu, J. Liu, J. Dai, S. An, S. Thibault, N. Walker, *Structure* **2013**, *21*, 798. <https://doi.org/10.1016/j.str.2013.02.025>
- [42] D. J. Gustin, Y. Li, M. L. Brown, X. Min, M. J. Schmitt, M. Wanska, X. Wang, R. Connors, S. Johnstone, M. Cardozo, A. C. Cheng, S. Jeffries, B. Franks, S. Li, S. Shen, M. Wong, H. Wesche, G. Xu, T. J. Carlson, M. Plant, K. Morgenstern, K. Rex, J. Schmitt, A. Coxon, N. Walker, F. Kayser, Z. Wang, *Bioorg. Med. Chem. Lett.* **2013**, *23*, 4608. <https://doi.org/10.1016/j.bmcl.2013.06.030>
- [43] J. A. Hengst, X. Wang, U. H. Sk, A. K. Sharma, S. Amin, J. K. Yun, *Bioorg. Med. Chem. Lett.* **2010**, *20*, 7498. <https://doi.org/10.1016/j.bmcl.2010.10.005>
- [44] L. Garuti, M. Roberti, G. Bottegoni, *Curr. Med. Chem.* **2014**, *21*, 2284. <https://doi.org/10.1016/j.ejmech.2016.12.010>
- [45] W. Akhtar, M. F. Khan, G. Verma, M. Shaquiquzzaman, M. Rizvi, S. H. Mehdi, M. Akhter, M. M. Alam, *Eur. J. Med. Chem.* **2017**, *126*, 705. <https://doi.org/10.1016/j.ejmech.2016.12.014>
- [46] M. J. Akhtar, A. A. Siddiqui, A. A. Khan, Z. Ali, R. P. Dewangan, S. Pasha, M. S. Yar, *Eur. J. Med. Chem.* **2017**, *126*, 853. <https://doi.org/10.1016/j.bbali.2012.07.002>
- [47] P. Singla, V. Luxami, K. Paul, *RSC Adv.* **2014**, *4*, 12422. <https://doi.org/10.1039/C3RA46304>
- [48] S. A. Galal, M. Khattab, S. A. Shouman, R. Ramadan, O. M. Kandil, O. M. Kandil, A. Tabll, Y. S. El Abd, R. El-Shenawy, Y. M. Attia, A. A. El-Rashedy, H. I. El Diwan, *Eur. J. Med. Chem.* **2018**, *146*, 687. <https://doi.org/10.1016/j.ejmech.2018.01.072>
- [49] S. A. Galal, S. H. Khairat, H. I. Ali, S. A. Shouman, Y. M. Attia, M. M. Ali, A. E. Mahmoud, A. H. Abdel-Halim, A. A. Fyiad, A. Tabll, R. El-Shenawy, Y. S. El Abd, R. Ramdan, H. I. El Diwani, *Eur. J. Med. Chem.* **2018**, *144*, 859. <https://doi.org/10.1016/j.ejmech.2017.12.023>
- [50] S. A. Galal, A. S. Abdelsamie, S. A. Shouman, Y. M. Attia, H. I. Ali, A. Tabll, R. El-Shenawy, Y. S. El Abd, M. M. Ali, A. E. Mahmoud, A. H. Abdel-Halim, A. A. Fyiad, A. S. Girgis, H. I. El Diwani, *Eur. J. Med. Chem.* **2017**, *134*, 392. <https://doi.org/10.1016/j.ejmech.2017.03.090>
- [51] M. A. Abdullaziz, H. T. Abdel-Mohsen, A. M. El Kerdawy, F. A. Ragab, M. M. Ali, S. M. Abu-Bakr, A. S. Girgis, H. I. El Diwani, *Eur. J. Med. Chem.* **2017**, *136*, 315. <https://doi.org/10.1016/j.ejmech.2017.04.068>
- [52] K. J. Flanagan, Y. M. Shaker, A. Temirak, H. I. El Diwani, *Heterocycles* **2015**, *91*, 1603. <https://doi.org/10.2987/COM-15-13258>
- [53] Y. M. Shaker, M. A. Omar, K. Mahmoud, S. M. Elhallouty, W. M. El-Senousy, M. M. Ali, A. E. Mahmoud, A. H. Abdel-Halim, S. M. Soliman, H. I. El Diwani, *J. Enzyme Inhib. Med. Chem.* **2015**, *30*, 826. <https://doi.org/10.3109/14756366.2014.979344>
- [54] A. Temirak, Y. M. Shaker, F. A. Ragab, M. M. Ali, S. M. Soliman, J. Mortier, G. Wolber, H. I. Ali, H. I. El Diwani, *Arch. Pharm.* **2014**, *347*, 291. <https://doi.org/10.1002/ardp.201300356>
- [55] A. Temirak, Y. M. Shaker, F. A. Ragab, M. M. Ali, H. I. Ali, H. I. El Diwani, *Eur. J. Med. Chem.* **2014**, *87*, 868. <https://doi.org/10.1016/j.ejmech.2014.01.063>
- [56] S. A. Galal, S. H. Khairat, F. A. Ragab, A. S. Abdelsamie, M. M. Ali, S. M. Soliman, J. Mortier, G. Wolber, H. I. El Diwani, *Eur. J. Med. Chem.* **2014**, *86*, 122. <https://doi.org/10.1016/j.ejmech.2014.08.048>
- [57] S. A. Galal, A. S. Abdelsamie, S. M. Soliman, J. Mortier, G. Wolber, M. M. Ali, H. Tokuda, N. Suzuki, A. Lida, R. A. Ramadan, H. I. El Diwani, *Eur. J. Med. Chem.* **2013**, *69*, 115. <https://doi.org/10.1016/j.ejmech.2014.08.048>
- [58] W. L. Santos, K. R. Lynch, *ACS Chem. Biol.* **2015**, *10*, 225. <https://doi.org/10.1016/j.ejmech.2013.07.049>
- [59] M. R. Pitman, M. Costabile, S. M. Pitson, *Cell. Signal.* **2016**, *28*, 1349. <https://doi.org/10.1016/j.cellsig.2016.06.007>
- [60] R. Prajuli, J. Banerjee, H. Khanal, *J. Chem.* **2015**, *31*, 2099. <https://doi.org/10.13005/ojc/310430>
- [61] E. Dikumar, V. Potkin, N. Kozlov, *Russ. J. Gen. Chem.* **2009**, *79*, 258. <https://doi.org/10.1134/S1070363209020157>
- [62] C. Rabong, C. Hametner, K. Mereiter, V. Kartsev, U. Jordis, *Heterocycles* **2008**, *75*, 799.
- [63] H. J. Park, K. Lee, S. J. Park, B. Ahn, J. C. Lee, H. Cho, K. I. Lee, *Bioorg. Med. Chem. Lett.* **2005**, *15*, 3307. <https://doi.org/10.1016/j.bmcl.2005.03.082>
- [64] S. Roy, A. D. Mahapatra, T. Mohammad, P. Gupta, M. F. Alajmi, A. Hussain, M. Rehman, B. Datta, M. I. Hassan, *Pharmaceuticals* **2020**, *13*, 118. <https://doi.org/10.3390/ph13060118>
- [65] S. Roy, T. Mohammad, P. Gupta, R. Dahiya, S. Parveen, S. Luqman, G. M. Hasan, M. I. Hassan, *ACS Omega* **2020**, *5*, 21550. <https://doi.org/10.1021/acsomega.0c02165>
- [66] P. Gupta, T. Mohammad, R. Dahiya, S. Roy, O. M. A. Noman, M. F. Alajmi, A. Hussain, M. I. Hassan, *Sci. Rep.* **2019**, *9*, 1. <https://doi.org/10.1038/s41598-019-55199-3>
- [67] P. Gupta, T. Mohammad, P. Khan, M. F. Alajmi, A. Hussain, M. T. Rehman, M. I. Hassan, *Biomed. Pharmacother.* **2019**, *118*, 109245. <https://doi.org/10.1038/s41598-019-55199-3>
- [68] National Cancer Institute, Developmental Therapeutic Program, www.dtp.nci.nih.gov
- [69] G. M. Morris, R. Huey, W. Lindstrom, M. F. Sanner, R. K. Belew, D. S. Goodsell, A. J. Olson, *J. Comput. Chem.* **2009**, *30*, 2785. <https://doi.org/10.1002/jcc.21256>
- [70] L. L. C. Schrodinger. The PyMOL Molecular Graphics System, **2015**, Version 1.8.
- [71] P. Gupta, F. I. Khan, S. Roy, S. Anwar, R. Dahiya, M. F. Alajmi, A. Hussain, M. T. Rehman, D. Lai, M. I. Hassan, *Spectrochim. Acta, Part A* **2020**, *225*, 117453. <https://doi.org/10.1016/j.saa.2019.117453>
- [72] K. A. Bakar, S. R. Feroz, *Spectrochim. Acta, Part A* **2019**, *223*, 117337. <https://doi.org/10.1016/j.saa.2019.117337>
- [73] H. Boaz, G. Rollefson, *J. Am. Chem. Soc.* **1950**, *72*, 3435.

SUPPORTING INFORMATION

Additional Supporting Information may be found online in the supporting information tab for this article.

How to cite this article: S. H. M. Khairat, M. A. Omar, F. A. F. Ragab, S. Roy, A. A. Turab Naqvi, A. S. Abdelsamie, A. K. H. Hirsch, S. A. Galal, M. I. Hassan, H. I. El Diwani, *Arch. Pharm.* **2021**;e2100080. <https://doi.org/10.1002/ardp.202100080>